doi: 10.12029/gc20190607

王旭辉, 郎兴海, 邓煜霖, 谢富伟, 娄渝明, 张赫, 杨宗耀. 2019. 西藏拉萨地体南缘汤白地区始新世辉绿岩脉——新特提斯洋壳断离的证据[J]. 中国地质, 46(6):1336−1355 .

Wang Xuhui, Lang Xinghai, Deng Yulin, Xie Fuwei, Lou Yuming, Zhang He, Yang Zongyao. 2019. Eocene diabase dikes in the Tangbai area, southern margin of Lhasa terrane, Tibet: Evidence for the slab break−off of the Neo−Tethys Ocean[J]. Geology in China, 46(6): 1336−1355(in Chinese with English abstract).

西藏拉萨地体南缘汤白地区始新世辉绿岩脉——新特提斯洋壳断离的证据

王旭辉[1],郎兴海[1],邓煜霖[1],谢富伟[1],娄渝明[1],张赫[1],杨宗耀[2]

(1.成都理工大学地球科学学院, 自然资源部构造成矿成藏重点实验室, 四川 成都 610059;
2.西南交通大学地球科学与环境工程学院, 四川 成都 611756)

提要:拉萨地体南缘汤白地区广泛分布新生代的辉绿岩脉。为探讨该辉绿岩脉形成时代、岩石成因和地质意义,对其开展了详细的岩相学、地球化学、锆石U−Pb年代学及Hf同位素研究。LA−ICP−MS锆石U−Pb定年结果显示辉绿岩脉的结晶年龄为(54±1)Ma,表明其形成于早始新世。微量元素地球化学特征显示富集大离子亲石元素(LILEs:如Rb、Sr和Ba),亏损高场强元素(HFSEs:如Nb、Ta和Ti)。与典型的弧岩浆岩、区域上叶巴组和桑日岩群中的玄武岩相比具有较高的Nb、TiO_2和Zr含量,在微量元素构造环境判别图解中显示出板内玄武岩地球化学属性。微量元素地球化学特征结合锆石Hf同位素表明岩浆源区除被俯冲板片释放的流体交代的岩石圈富集地幔外,还有软流圈亏损地幔物质加入。汤白辉绿岩脉侵入年龄与区域上林子宗群火山活动峰期接近(52 Ma)。同时结合岩石成因及构造背景,作者认为汤白辉绿岩脉是54~52 Ma新特提斯洋壳断离诱发岩浆作用的产物。根据最新大陆碰撞及板片断离的三维数值模型,暗示了印度板块与欧亚大陆碰撞的起始时间为65 Ma或者更早。

关 键 词:拉萨地体;辉绿岩脉;构造背景;板片断离;印度−欧亚大陆碰撞;地质调查工程;西藏

中图分类号:P581;P597+.3 **文献标志码**:A **文章编号**:1000−3657(2019)06−1336−20

Eocene diabase dikes in the Tangbai area, southern margin of Lhasa terrane, Tibet: Evidence for the slab break−off of the Neo−Tethys Ocean

WANG Xuhui[1], LANG Xinghai[1], DENG Yulin[1], XIE Fuwei[1], LOU Yuming[1], ZHANG He[1], YANG Zongyao[2]

(1. *MNR Key Laboratory of Tectonic Controls on Mineralization and Hydrocarbon Accumulation, College of Earth Science, Chengdu University of Technology, Chengdu* 610059*, Sichuan, China;* 2. *Faculty of Geosciences and Environmental Engineering, Southwest Jiaotong University, Chengdu* 611756*, Sichuan, China*)

收稿日期:2018−09−07;**改回日期**:2019−01−10

基金项目:国家重点研发计划课题(2018YFC0604105),国家自然科学基金项目(41502079、41972084),中国地质调查局项目(DD20160346),西北大学大陆动力学国家重点实验室开放课题基金项目(18LCD04)及深地资源成矿作用与矿产预测重点实验室开放基金项目(ZS1911)联合资助。

作者简介:王旭辉,男,1993年生,博士生,矿物学、岩石学、矿床学专业;E−mail:wangxuhui618@126.com。

通讯作者:郎兴海,男,1982年生,博士生导师,教授,主要从事矿床学、矿产普查与勘探方面的研究;E−mail:langxinghai@126.com。

Abstract: Diabase dikes are extensively distributed in the Tangbai area on the southern margin of the Lhasa terrane. In order to discuss their formation age, genesis and tectonic implications, the authors investigated their petrography, geochemistry, zircon U−Pb geochronology and Hf isotope. Zircon U−Pb dating yielded an age of (54±1) Ma for the Tangbai diabase dikes, indicating that they were formed in the Early Eocene. The trace elements are characterized by enrichment of LILEs (such as Rb, Sr and Ba) and depletion of HFSEs (such as Nb, Ta and Ti). Compared with typical arc magmas, Sangri Group basalts and Yeba Formation basalts in this area, the Tangbai diabase dikes have higher values of Nb, TiO_2 and Zr. Trace element tectonic discrimination diagrams show that Tangbai diabase dikes fall in intraplate basalts field, and show geochemical affinities with intraplate magmatism. The race element geochemical characteristics and zircon Hf isotopic data suggest that the diabase dikes were likely derived from enriched lithospheric mantle which had been metasomatized by slab−derived fluids during previous subductions, and mixed with upwelling ashospheric mantle. The intrusion age of Tangbai diabase dikes was close to the peak period (52 Ma) of Linzizong volcanic activity. Combined with their genesis and tectonic setting, the authors hold that the formation of the Tangbai diabase dikes was related to slab break−off of the northward subduction of the Neo−Tethyan slab ca. 54~52 Ma in age. In addition, according to the latest 3−D numerical models of continental collision and slab break−off, it is shown that the onset of India−Eurasia continental collision should have occurred at 65 Ma or earlier.

Key words: Lhasa terrane; diabase dikes; tectonic setting; slab break− off; India−Eurasia continental collision;geological survey engineering;Tibet

About the first author: WANG Xuhui, male, born in 1993, doctor candidate, majors in mineralogy, petrology, and mineral deposit geology; E−mail: wangxuhui618@126.com.

About the corresponding author: LANG Xinghai, male, born in 1982, professor, supervisor of doctoral candidates, engages in research on economic geology and mineral exploration; E−mail: langxinghai@126.com.

Fund support: Supported by the National Key R&D Program of China (2018YFC0604105), National Natural Science Foundation of China (41502079, 41972084), China Geological Survey Programs (DD20160346), the Opening Foundation of State Key Laboratory of Continental Dynamics, Northwest University (18LCD04), and the Opening Foundation of MNR Key Laboratory of Metallogeny and Mineral Assessment (ZS1911).

1 引 言

新特提斯洋开启—俯冲消亡、印度板块与欧亚板块碰撞以及青藏高原的快速隆升是地球演化史上一次重大地质事件,一直以来备受地质学家们的关注。近年来国内外学者对拉萨地体的中—新生代构造演化过程和岩浆事件进行了大量的研究,并取得了显著的成果(Chung et al., 2005; Chu et al., 2006; Mo et al., 2007, 2008; Wen et al., 2008; Ji et al., 2009b; Zhu et al., 2011, 2013, 2015; Pan et al., 2012; Lang et al., 2014; Kang et al., 2014; Meng et al., 2016;尹滔等,2019)。但在一些关键问题上仍存在分歧,如印度板块与欧亚大陆碰撞的时间究竟是何时开始的,一些学者认为早于55 Ma(Jaeger et al., 1989; Liu and Einsele, 1994; Yin and Harrison, 2000;莫宣学等, 2003, 2007; Leech et al., 2005; Xu et al., 2008; 黄宝春等, 2010),然而另一些学者认为晚于55 Ma(Searle et al., 1987; Dewey et al., 1989; Aitchison, 2007)。为了探明这一问题,地质学者对拉萨地体上广泛分布的新生代中酸性岩浆岩做了大量的研究(Chung et al., 2003, 2005; Ding et al., 2003; Mo et al., 2007, 2008; Ji et al., 2009a, 2009b; Zhao et al., 2009; Lee et al., 2009, 2012; Gao et al., 2010; Chu et al., 2011),此外也有少量同时期的基性岩脉报道(高永丰等, 2006; 岳雅慧和丁林, 2006; Xu et al., 2008; 刘立文等, 2012; 贾黎黎等, 2013; Huang et al., 2017)。基性岩脉通常起源于岩石圈地幔或软流圈地幔,是拉张构造背景的典型产物(Holm et al., 2006; Ernst et al., 2008; Hou et al., 2008; Wu et al., 2014; Cui et al., 2015),其蕴含着丰富的关于岩浆源区、运动及动力学信息(Hoek and Seitz, 1995; Gladkochub et al., 2006; Pisarevsky and Bylund, 2006; Ernst et al., 2008; Hou et al., 2008; Boekhout et al., 2012),是窥探地球内部结构构造和物质能量交换最理想的"探针"或"窗口",例如安第斯山大量中生代基性岩脉的存在帮助地质学家们理解泛大陆的裂解(Boekhout et al., 2012)。基于这一事实,本文在对拉萨地体南缘汤白辉绿岩脉开展

了详细的野外地质调查基础上，进一步开展了岩相学、地球化学、锆石U−Pb年代学以及Hf同位素研究。探讨了辉绿岩脉形成的时间、地质构造背景和岩石成因，同时结合区域上前人研究的成果和最新大陆碰撞及板片断离的三维数值模型试图对印度板块与欧亚大陆碰撞的起始时间做出进一步的约束。

2 地质背景

研究区位于拉萨地体中段南缘日喀则市汤白村境内(图1b)，拉萨地体是夹持于班公湖—怒江缝合带(BNSZ)和雅鲁藏布江缝合带(YZSZ)之间一条近东西向的巨型构造−岩浆带，东西长约2500 km，南北宽150~300 km，面积约45万km^2(潘桂棠等, 2006)；根据其内部构造又可以进一步划分为3个亚带，即以狮泉河—纳木错蛇绿混杂岩带(SNMZ)和洛巴堆—米拉山断裂带(LMF)这两条近东西向的构造带为界，由北向南分别为北部拉萨地体、中部拉萨地体和南部拉萨地体(图1a，朱弟成

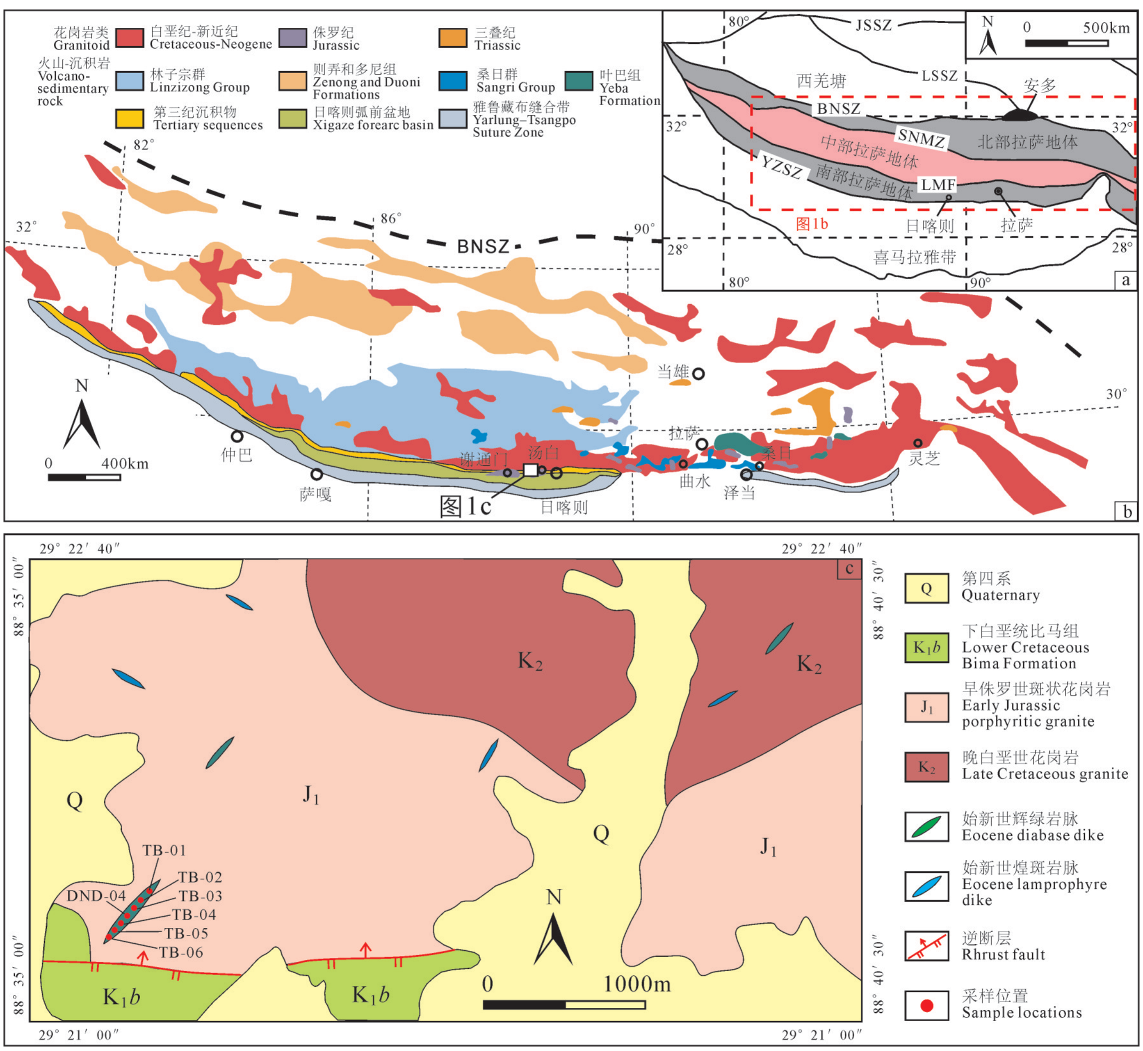

图1 拉萨地体构造划分图(a, Zhu et al., 2011)和岩浆岩分布图(b, Wang et al., 2016)及汤白研究区地质简图(c,据唐菊兴等, 2005)

JSSZ—金沙江缝合带；LSSZ—龙木错—双湖缝合带；BNSZ—班公湖—怒江缝合带；YZSZ—雅鲁藏布缝合带；SNMZ—狮泉河—纳木错混杂岩带；LMF—洛巴堆—米拉山断裂带

Fig.1 Tectonic framework (a, after Zhu et al., 2011) and magmatic rocks distribution (b, after Wang et al., 2016) in the Lhasa terrane and geological map of Tangbai area (c, after Tang et al., 2005)

JSSZ−Jinshajiang Suture Zone；LSSZ−Longmu Tso−Shuanghu Suture Zone；BNSZ−Bangong−Nujiang Suture Zone；YZSZ−Yarlung−Zangbo Suture Zone；SNMZ−Shiquan River−Nam Tso Mélange Zone；LMF−Luobadui−Milashan Fault

等, 2012)。其中北部和中部拉萨地体总体相似,上覆火山-沉积地层被大量的中生代花岗岩类侵入(图1b,潘桂棠等, 2006; Zhu et al., 2013);不同之处在于北部拉萨地体以新生地壳为主(张立雪等, 2013; Hou et al., 2015),而中部拉萨地体发育寒武纪或新元古代结晶基底(Xu et al., 1985; Guynn et al., 2006)。南拉萨地体记录了新特提斯洋向北俯冲以及印度—亚洲大陆碰撞造山有关的构造岩浆演化和成矿作用信息,显示出新生地壳特征(张立雪等, 2013; Hou et al., 2015),在东部可能存在结晶基底(Dong et al., 2010; Zhu et al., 2013),其上广泛发育晚三叠世—中新世的岩浆岩;其中以白垩纪—新近纪冈底斯岩基和古近纪林子宗火山岩为主(图1b,Zhu et al., 2013),中生代沉积岩零星发育(潘桂棠等, 2006),同时在南拉萨地体还发育有中新世的埃达克岩、钾质和超钾质岩石(Hou et al., 2004; Wen et al., 2008; Zhu et al., 2009; Zheng et al., 2012; Tian et al., 2017)。

3　样品特征及测试方法

3.1 样品特征

研究区出露的岩浆岩主要有早侏罗世斑状花岗岩、晚白垩世花岗岩以及始新世的辉绿岩脉和煌斑岩脉(图1c)。辉绿岩脉呈陡倾脉状侵入到早侏罗世斑状花岗岩(190 Ma,王旭辉等,2018)和晚白垩世花岗岩中(图1c)。早侏罗世斑状花岗岩显示出块状构造和似斑状结构(图2b),斑晶含量约为75%,主要由石英(30%)、斜长石(30%)和碱性长石(15%)组成;基质含量约25%,由一些细粒的微晶构成,主要为斜长石、碱性长石、石英和少量角闪石。辉绿岩脉与围岩接触界线清楚,延伸方向近北东向,脉宽5~20 m不等。研究样品采集于南侧侵位于早侏罗世斑状花岗岩中最宽、最长的一条脉体。采样地理坐标为:29°21′51″N,88°35′29″E,样品沿脉体的延伸方向依次采集。南侧出露的地层为下白垩统比马祖(K_1b),主要为一套火山-沉积岩组合,火山岩主要类型为玄武安山岩、安山岩、英安岩和条带状变质凝灰岩等;沉积岩主要为灰白色中层砂岩夹薄层状粉砂岩、页岩,岩石普遍受低级变质作用改造(唐菊兴等, 2005)。

辉绿岩脉野外出露良好,风化面呈红褐色、灰色,新鲜面呈灰绿色(图2a、c)。镜下可见细粒晶质结构和辉绿结构(图2e、f),斜长石含量大于50%,粒径0.1~1.0 mm不等,半自形厚板状或条状,具有较宽的聚片双晶条纹(图2e),显示出基性斜长石特征,采用微晶消光角法测的斜长石主要为拉长石,其遭受了弱的绢云母化和黏土化。辉石含量30%~40%,以斜消光和最高干涉色为二级紫红色为特征,属于单斜辉石,粒径一般小于0.4 mm,呈他形粒状充填于斜长石框架的空隙中,构成典型辉绿结构(图2e、f),边缘常发生绿泥石和纤闪石蚀变。含有少量(<5%)较粗的橄榄石颗粒,呈半自形粒状,被细粒斜长石包围,粒径约0.2 mm(图2f),蚀变较弱。角闪石含量较少,少于5%,他形粒状,发育绿泥石化等次生变化,还含有少量的磁铁矿、榍石和锆石等副矿物。经过详细的野外观察和室内镜下鉴定,本次共选取有代表性的组构清晰、蚀变弱的7件辉绿岩脉样品用于研究,其中1件用于锆石U-Pb年代学研究,另外6件用于岩石地球化学研究。

3.2 测试方法

选取一件重50 kg具有代表性的样品在河北省廊坊市科大岩石矿物分选技术服务有限公司完成锆石单矿物的挑选,锆石的制靶及照相在北京锆年领航科技有限公司完成。根据锆石的透射光、反射光和阴极发光图像,尽量选择锆石表面无裂痕,内部无包裹体和环带结构清晰位置作为测试点。利用LA-ICP-MS进行锆石U-Pb同位素分析。测试在西北大学大陆动力学国家重点实验室完成。其中,LA-ICP-MS分析在Hewlett Packard公司带有Shield Torch的Agilient 7500a ICP-MS和德国Lambda Physik公司的ComPex102 Excimer激光器(工作物质ArF,波长193 nm)以及MicroLas公司的Geolas 200 M光学系统的联机上进行。激光束斑直径为30 μm,激光剥蚀样品的深度为20~40 μm。实验中采用He作为剥蚀物质的载气。锆石年龄采用国际标准锆石91500作为外标标准物质,测试过程中在每测定5个样品重复测定一个锆石91500对样品进行校正,并测量一个锆石Plesovice,观察仪器的状态和测试的重现性。样品的同位素比值及元素含量计算采用Glitter(ver4.0,Macquarie University)程序,年龄计算及谐和图的绘制用Isoplot 4.15完成。详细分析步骤和数据处理方法见文献(Yuan et al., 2004, 2008)。

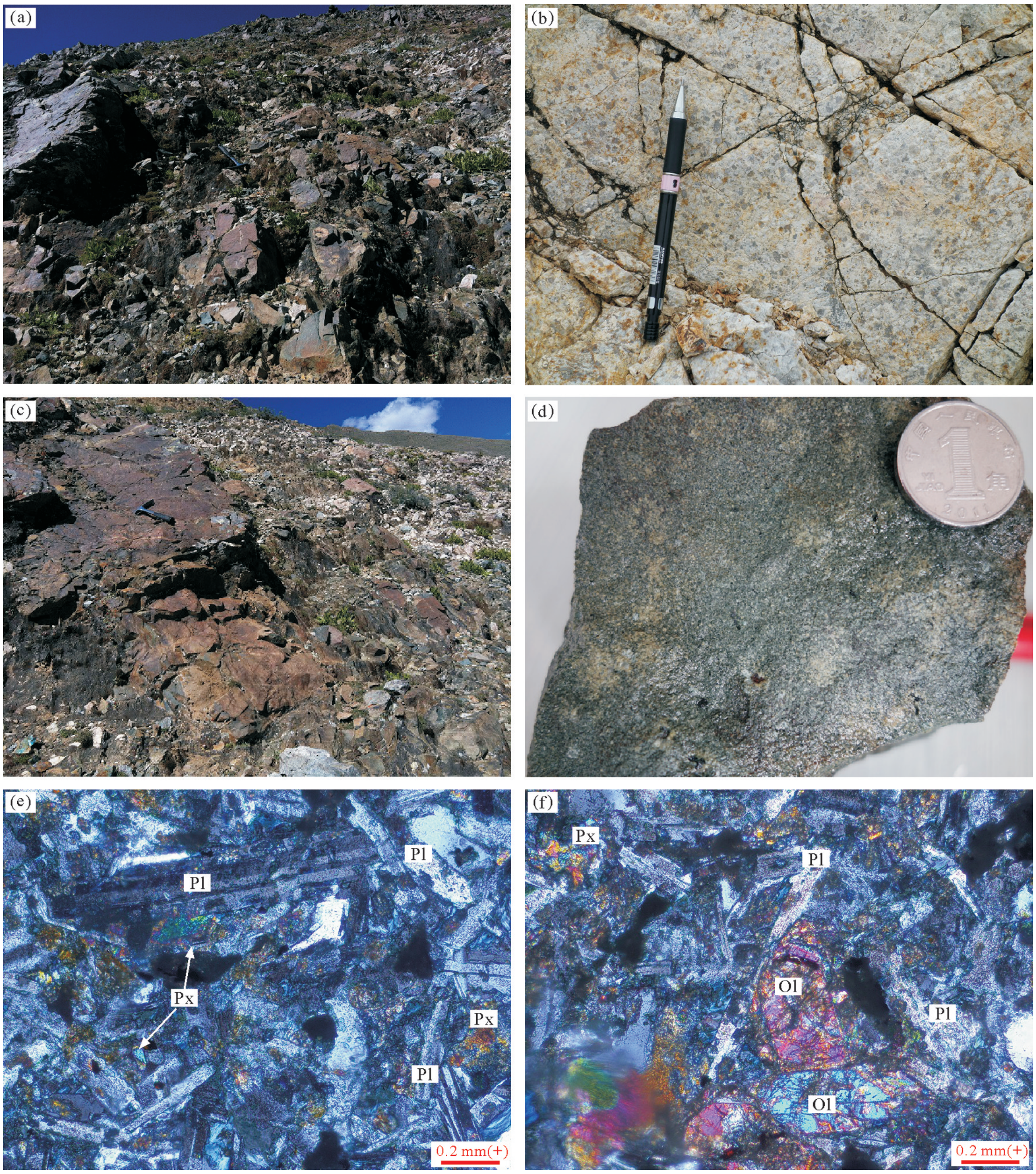

图2 汤白辉绿岩脉及其围岩野外露头及显微照片
Px—辉石；Pl—斜长石；Ol—橄榄石
Fig. 2 Photos of fields and microphotographs of the Tangbai diabase dikes
Px-Pyroxene; Pl-Plagioclase; Ol-Olivine

锆石Hf同位素测试是在北京科荟测试技术有限公司Neptune plus多接收等离子质谱及配套的ESI NWR193紫外激光剥蚀系统(LA-MC-ICP-MS)上进行的，实验过程中采用He作为剥蚀物质载气，剥蚀直径采用50 μm，测定时使用锆石国际标样GJ1作为参考物质，分析点与U-Pb定年分析点为同一位置。相关仪器运行条件及详细分析流程见侯可军等(2007)。分析过程中锆石标准GJ1的^{176}Hf/^{177}Hf测试加权平均值为0.282007±0.000007，与文献报道值(Morel et al., 2006)在误差范围内完全一致。

主量元素、微量元素分析在西南冶金地质测试

中心进行。主量元素测试采用X射线荧光光谱法(XRF),在荷兰帕纳科Axios X荧光仪完成,分析误差优于3%。微量元素测定采用电感耦合等离子体质谱法(ICP−MS),在NexIon 300x ICP−MS仪器上完成,将样品研磨并用酸溶法制成溶液,然后在等离子质谱仪上进行测定,并用标准溶液进行校正,含量大于10×10^{-6}的元素分析误差小于5%,而含量小于10×10^{-6}的元素分析误差小于10%。

4 分析结果

4.1 锆石U−Pb年代学

本文对汤白辉绿岩脉进行LA−ICP−MS锆石U−Pb定年,辉绿岩脉样品(DND−04)锆石颗粒粒径变化较大(60~180 μm),具有自形—半自形晶形,长宽比在1∶1~1∶2,阴极发光(CL)图像显示绝大多数的锆石具有典型的岩浆震荡环带,环带中各分带之间的宽度较大(图3),呈现出基性岩浆锆石特征。本次共获得20个有效数据点,U含量为210×10^{-6}~2125×10^{-6},Th含量为135×10^{-6}~2437×10^{-6},相应的Th/U比值为0.48~1.18,且Th与U存在正相关关系,显示所测的锆石为岩浆成因(Hoskin and Blaek, 2000)。锆石颗粒在谐和曲线附近构成一个年龄集中区,其$^{206}Pb/^{238}U$年龄范围为51~57 Ma(表1,图4),加权平均年龄值为(54±1) Ma(MSWD=1.2),该年龄代表辉绿岩脉的结晶年龄,表明辉绿岩脉的形成时代为早始新世。

4.2 锆石Hf同位素

对汤白辉绿岩脉测年样品(DND−04)中的锆石Hf同位素测定成分结果列于表2,本次共测定了17颗锆石Hf同位素数据,所测锆石的$^{176}Lu/^{177}Hf$值较低(均值为0.0012),表明锆石在形成后具有极低的放射性成因Hf积累,因此所测定的$^{176}Hf/^{177}Hf$值可以代表锆石结晶时体系的Hf同位素组成(Amelin et al., 2000)。样品中17颗锆石的$^{176}Hf/^{177}Hf$值变化范围在0.282631~0.282991(表2),平均值为0.282824;对应的$\varepsilon_{Hf}(t)$值变化范围为−3.9~8.9(表2,图5),平均值为3.0;Hf同位素单阶段模式年龄(T_{DM1})和二阶段模式年龄(T_{DM2})分别为368~888 Ma和558~1374 Ma(表2)。

4.3 地球化学特征

共对6件辉绿岩脉样品进行分析,分析的主微量元素含量列于表3。

汤白辉绿岩脉样品主量元素变化范围较小,SiO_2含量较高,为52.13%~52.58%;MgO和TiO_2含量中等,分别为3.14%~3.66%和0.97%~1.02%;$Mg^{\#}$值为38~42,平均值为41,低于原始岩浆$Mg^{\#}$值(>65, Wilson, 1989);具有富钠(Na_2O=2.31%~3.22%)、贫钾(K_2O=0.38%~0.96%)特征。在TAS图解上(图6a),6个样品均落在辉长岩边界上,与野外观察和室内镜下鉴定结果一致;在SiO_2−TFeO/MgO图解上(图6b),所有样品落在拉斑系列区域。

汤白辉绿岩脉稀土元素总量(ΣREE)为69.09×10^{-6}~77.79×10^{-6},平均值73.96×10^{-6}。其中轻稀土含量(ΣLREE)为56.72×10^{-6}~64.47×10^{-6},平均值60.86×10^{-6};重稀土含量(ΣHREE)为12.38×10^{-6}~13.57×10^{-6},平均值13.10×10^{-6};$(La/Yb)_N$=3.90~4.58,平均值4.26。稀土元素球粒陨石标准化配分图(图7a)显示,轻稀土元素富集,重稀土元素亏损,呈右倾趋

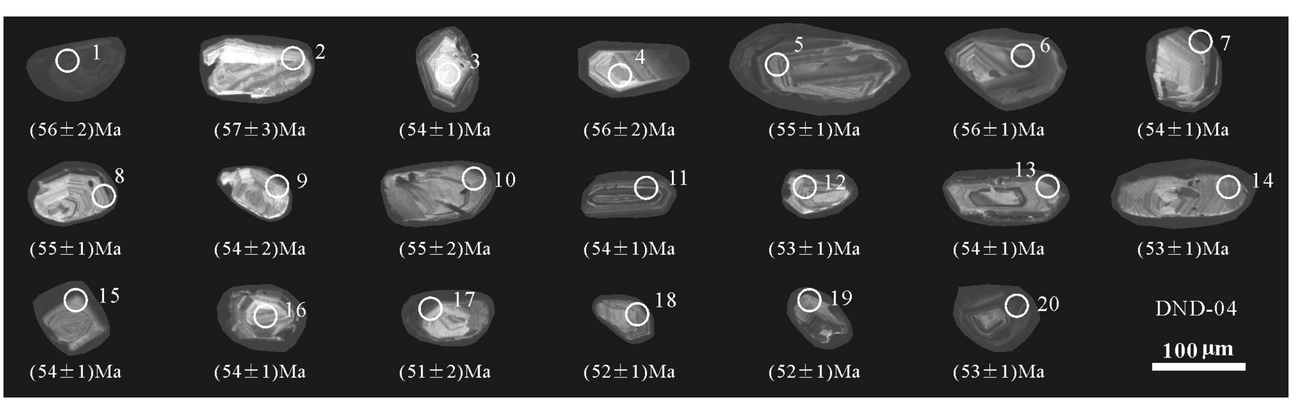

图3 汤白辉绿岩脉样品锆石的阴极发光图像

Fig.3 Cathodoluminescene images of zircons from the Tangbai diabase dikes

表1 汤白辉绿岩脉LA-ICP-MS锆石U-Pb测试结果

Table 1 LA-ICP-MS zircon U-Pb analysis data of the Tangbai diabase dikes

测点号	元素含量/10^{-6}			Th/U	同位素比值						年龄/Ma	
	U	Th	$^{206}Pb^*$		$^{207}Pb/^{206}Pb$	±1σ	$^{207}Pb/^{235}U$	±1σ	$^{206}Pb/^{238}U$	±1σ	$^{206}Pb/^{238}U$	±1σ
DND-04:辉绿岩(29°21′51″,88°35′29″)												
01	268	141	2.57	0.53	0.1190	0.0139	0.1298	0.0116	0.0087	0.0004	56	2
02	331	215	3.47	0.65	0.1515	0.0228	0.1514	0.0164	0.0088	0.0004	57	3
03	309	213	2.83	0.69	0.1008	0.0062	0.1109	0.0065	0.0085	0.0002	54	1
04	281	135	2.75	0.48	0.1287	0.0240	0.1341	0.0168	0.0087	0.0004	56	2
05	685	483	6.56	0.71	0.0659	0.0044	0.0755	0.0048	0.0086	0.0002	55	1
06	639	456	6.80	0.71	0.1254	0.0081	0.1496	0.0093	0.0087	0.0002	56	1
07	363	303	3.57	0.84	0.1075	0.0088	0.1140	0.0079	0.0084	0.0002	54	1
08	324	237	3.25	0.73	0.1012	0.0067	0.1120	0.0063	0.0086	0.0002	55	1
09	210	223	2.16	1.06	0.1217	0.0162	0.1226	0.0081	0.0084	0.0003	54	2
10	339	221	3.64	0.65	0.1198	0.0165	0.1395	0.0184	0.0086	0.0003	55	2
11	2125	2437	22.89	1.15	0.0496	0.0017	0.0573	0.0019	0.0084	0.0001	54	1
12	420	493	4.51	1.18	0.0878	0.0038	0.0962	0.0039	0.0083	0.0001	53	1
13	569	537	5.87	0.94	0.0722	0.0036	0.0805	0.0038	0.0084	0.0001	54	1
14	390	329	3.89	0.84	0.0764	0.0041	0.0834	0.0039	0.0083	0.0002	53	1
15	331	211	3.17	0.64	0.1118	0.0081	0.1131	0.0054	0.0084	0.0002	54	1
16	263	302	2.77	1.15	0.0978	0.0066	0.1084	0.0061	0.0084	0.0002	54	1
17	436	458	4.31	1.05	0.0955	0.0076	0.0981	0.0073	0.0079	0.0003	51	2
18	791	751	7.49	0.95	0.0550	0.0035	0.0607	0.0038	0.0081	0.0002	52	1
19	1114	1229	11.06	1.10	0.0542	0.0033	0.0610	0.0040	0.0081	0.0001	52	1
20	874	880	8.69	1.01	0.0637	0.0032	0.0694	0.0031	0.0083	0.0001	53	1

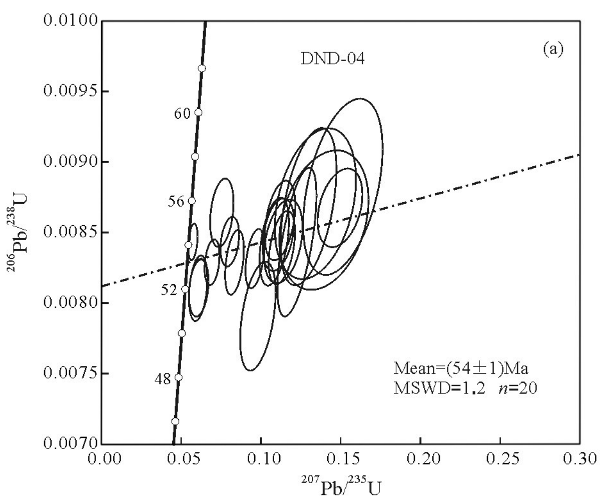

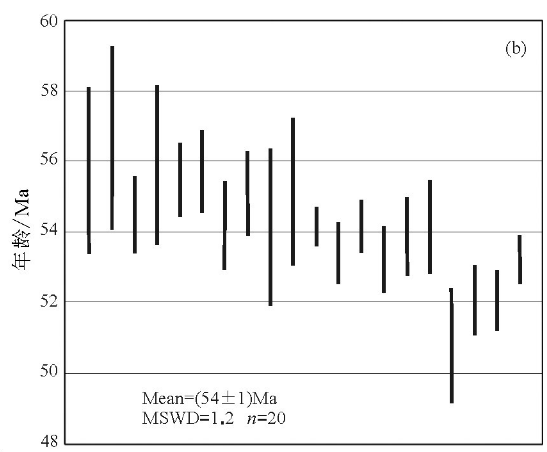

图4 汤白辉绿岩脉锆石U-Pb谐和图(a)及$^{206}Pb/^{238}U$加权平均年龄图(b)

Fig.4 U-Pb concordant diagram (a) and $^{206}Pb/^{238}U$ weighted average age diagram (b) of zircon grains from the Tangbai diabase dikes

势。Eu正异常微弱,5个样品的δEu>1(1.03~1.08),仅TB-03样品的δEu<1(0.96),指示斜长石的分异结晶作用较弱。

汤白辉绿岩脉微量元素原始地幔标准化蛛网图显示出其配分模式整体向右倾斜,相对富集大离子亲石元素(LILEs:如Rb、Sr和Ba)和亏损高场强元素(HFSEs:如Nb、Ta和Ti)(图7b),与典型的弧岩浆岩微量元素原始地幔标准化配分模式相比而言,

表2 汤白辉绿岩脉锆石Lu-Hf同位素测试结果

Table 2 Lu-Hf isotopic compositions of zircons from the Tangbai diabase dikes

测点号	$^{176}Yb/^{177}Hf$	±2δ	$^{176}Lu/^{177}Hf$	±2δ	$^{176}Hf/^{177}Hf$	±2δ	t/Ma	$\varepsilon_{Hf}(0)$	$\varepsilon_{Hf}(t)$	T_{DM1}/Ma	T_{DM2}/Ma	$f_{Lu/Hf}$
DND-04:辉绿岩(29°21′51″,88°35′29″)												
02	0.027166	0.000256	0.001181	0.000009	0.282683	0.000032	57	-3.2	-1.9	810	1255	-0.96
03	0.028165	0.000606	0.001192	0.000025	0.282815	0.000028	54	1.5	2.7	622	957	-0.96
04	0.028772	0.000460	0.001232	0.000017	0.282862	0.000018	56	3.2	4.3	557	852	-0.96
05	0.025967	0.000351	0.001141	0.000017	0.282948	0.000017	55	6.2	7.4	432	655	-0.97
06	0.027133	0.000317	0.001183	0.000013	0.282939	0.000017	56	5.9	7.1	446	676	-0.96
07	0.021502	0.000054	0.000929	0.000001	0.282808	0.000018	54	1.3	2.4	628	973	-0.97
08	0.016283	0.000251	0.000789	0.000015	0.282991	0.000020	55	7.7	8.9	368	558	-0.98
09	0.025218	0.000283	0.001095	0.000011	0.282827	0.000019	54	2.0	3.1	604	931	-0.97
10	0.021213	0.000724	0.000905	0.000028	0.282692	0.000020	55	-2.8	-1.7	792	1236	-0.97
11	0.078497	0.000605	0.003148	0.000005	0.282795	0.000028	54	0.8	1.9	687	1008	-0.91
12	0.033940	0.000527	0.001454	0.000021	0.282917	0.000020	53	5.1	6.2	481	729	-0.96
13	0.050649	0.000333	0.002287	0.000010	0.282772	0.000021	54	0.0	1.1	704	1057	-0.93
14	0.031489	0.000566	0.001369	0.000024	0.282631	0.000019	53	-5.0	-3.9	888	1374	-0.96
15	0.023609	0.000139	0.001018	0.000006	0.282747	0.000017	54	-0.9	0.3	716	1112	-0.97
16	0.025279	0.000239	0.001196	0.000010	0.282731	0.000018	54	-1.4	-0.3	742	1148	-0.96
17	0.026212	0.000168	0.001188	0.000006	0.282968	0.000018	51	7.0	8.0	404	612	-0.96
20	0.025846	0.000411	0.001135	0.000022	0.282884	0.000018	53	4.0	5.1	523	801	-0.97

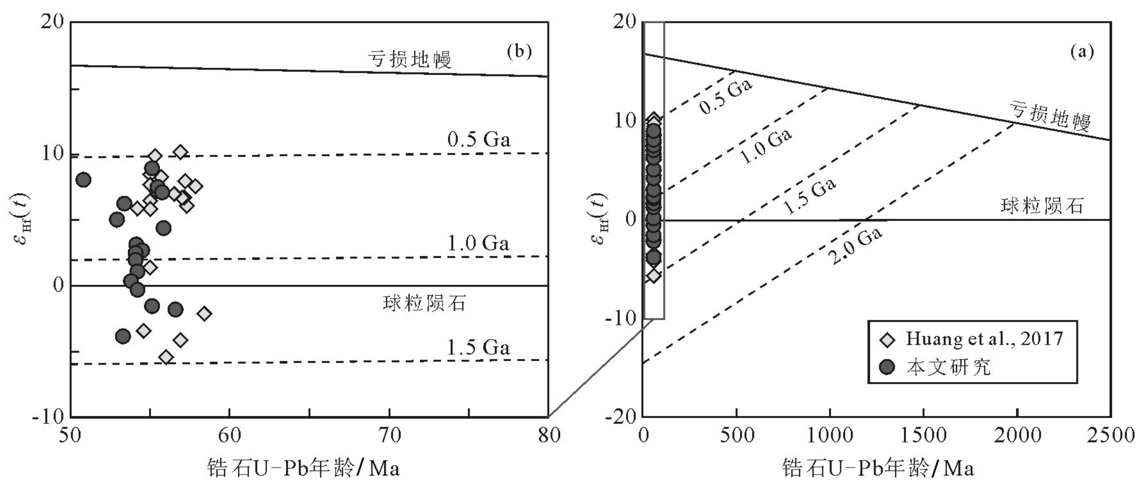

图5 汤白辉绿岩脉锆石$\varepsilon_{Hf}(t)$值与U-Pb年龄图解

Fig. 5 Plots of zircon U-Pb ages versus $\varepsilon_{Hf}(t)$ values of the Tangbai diabase dikes

其Nb、Ta和Ti亏损较弱(图7b)。

5 讨 论

5.1 时空分布特征

本文采用LA-ICP-MS锆石U-Pb测年的方法对拉萨地体中段南缘汤白辉绿岩脉样品进行年代学研究,获得的辉绿岩脉的结晶年龄为(54±1) Ma,与赵志丹等(2011)获得西藏当雄南部的辉长岩的LA-ICP-MS锆石U-Pb年龄一致(54 Ma);在拉萨地体中段南缘,Mo et al.(2005)获得拉萨—曲水一带辉长岩和基性暗色包体的年龄为47~51 Ma,日喀则—拉萨一带也有辉长岩SHRIMP锆石U-Pb年龄报道(Dong et al., 2005;董国臣等, 2008),其辉长岩的年龄值在50~52 Ma,最近Huang et al.(2017)在研究区的西侧达孜地区发现了大量的镁铁质岩脉,其形成时代为古新世末期(~57 Ma)。同样在拉萨北

表3 汤白辉绿岩脉主量元素(%)和微量元素(10^{-6})分析数据

Table 3 Major (%) and trace (10^{-6}) elements analyses of the Tangbai diabase dikes

样品号	TB-01	TB-02	TB-03	TB-04	TB-05	TB-06
岩性	辉绿岩(N29°21′51″;E88°35′29″)					
SiO_2	52.13	52.33	52.17	52.58	52.35	52.45
TiO_2	0.99	1.00	0.97	1.00	1.00	1.02
Al_2O_3	16.19	16.25	15.88	16.23	16.12	16.28
Fe_2O_3	3.98	4.09	5.19	4.41	3.95	4.42
FeO	5.42	5.37	4.44	5.11	5.50	5.08
MnO	0.18	0.18	0.17	0.17	0.18	0.18
MgO	3.64	3.57	3.14	3.54	3.66	3.52
CaO	8.19	8.30	10.54	7.96	8.11	8.36
Na_2O	3.16	3.22	2.31	3.21	3.22	3.15
K_2O	0.89	0.91	0.38	0.96	0.92	0.75
P_2O_5	0.21	0.21	0.21	0.21	0.21	0.21
LOI	4.32	3.92	3.91	3.93	4.16	3.96
Total	99.30	99.34	99.31	99.31	99.35	99.38
$Mg^{\#}$	42	41	38	41	42	41
Sc	30.62	39.59	35.65	38.52	40.53	38.34
V	267	281	282	286	275	287
Cr	42.51	40.21	41.94	40.20	40.57	43.92
Co	31.13	29.32	28.08	29.56	30.74	31.52
Ni	10.18	10.43	9.46	10.25	10.20	11.25
Cu	198	194	133	202	209	187
Zn	118.6	114.6	74.4	112.9	120.9	118.9
Ga	19.89	23.19	23.26	22.82	22.75	22.49
Rb	17.68	17.20	8.08	19.04	17.77	14.61
Sr	474	478	661	473	467	467
Y	19.17	17.71	19.31	18.00	19.57	19.06
Zr	98.84	100.26	99.46	98.92	97.90	100.09
Nb	4.01	4.46	4.44	4.54	4.49	4.34
Cs	0.57	0.69	0.31	0.96	0.70	0.62
Ba	296	317	122	355	324	261
La	12.41	10.71	11.46	11.35	12.05	11.12
Ce	26.25	23.04	24.73	23.97	25.77	24.12
Pr	3.81	3.36	3.64	3.47	3.74	3.59
Nd	16.93	14.95	16.38	15.78	16.75	16.16
Sm	3.81	3.46	3.75	3.58	3.86	3.75
Eu	1.26	1.20	1.16	1.24	1.31	1.25
Gd	3.56	3.27	3.52	3.36	3.61	3.51
Tb	0.60	0.56	0.60	0.56	0.61	0.59
Dy	3.74	3.52	3.78	3.53	3.87	3.74
Ho	0.77	0.72	0.79	0.74	0.78	0.78
Er	2.04	1.89	2.08	1.90	2.06	2.01
Tm	0.33	0.31	0.36	0.32	0.34	0.33
Yb	1.94	1.81	2.01	1.86	1.98	2.04
Lu	0.31	0.29	0.32	0.28	0.32	0.30
Hf	2.88	2.89	2.44	2.96	3.01	2.92
Ta	0.23	0.26	0.27	0.27	0.27	0.26
Pb	23.27	23.72	12.16	21.62	26.31	18.31
Th	1.54	1.81	1.91	1.88	1.94	1.71
U	0.58	0.65	0.67	0.68	0.67	0.64
Nb/Ta	17.14	17.05	16.39	16.92	16.65	16.54
Zr/Hf	34.32	34.69	40.76	33.42	32.52	34.28
Lu/Yb	0.16	0.16	0.16	0.15	0.16	0.15
ΣREE	77.79	69.09	74.59	71.95	77.04	73.29
ΣLREE	64.47	56.72	61.12	59.39	63.47	59.98
ΣHREE	13.32	12.38	13.47	12.56	13.57	13.30
$(La/Yb)_N$	4.58	4.25	4.08	4.37	4.37	3.90
δEu	1.03	1.07	0.96	1.08	1.05	1.04

部的林周盆地也有少量的基性岩脉的年龄报道(52.5 Ma,岳雅慧和丁林, 2006)。不难发现在拉萨地体中段拉萨至达孜一带均有基性侵入岩或基性暗色包体分布,其形成的时代集中在始新世早期。同时在该时间段(约52 Ma),林子宗火山活动达到峰期,在区域上自西向东形成了范围广泛、规模巨大的火山岩(图1b, Wen et al., 2008; Lee et al., 2009),说明在时间序列上这些基性岩浆岩与林子宗火山活动是同一时期岩浆作用的产物。

5.2 构造背景

辉绿岩脉稀土元素配分模式呈现右倾模式,微量元素原始地幔标准化蛛网图显示出Nb和Ta相对亏损(图7a、b),表现出与弧岩浆岩相似的特征。除此之外,辉绿岩脉的一些地球化学特征不同于典型弧岩浆岩而与板内伸展背景下玄武岩地球化学特征相似。

典型弧岩浆岩具有较低的TiO_2和Nb含量,分别小于1%和2×10^{-6}(Martin et al., 2005)。区域上叶巴组和桑日群火山岩是典型的弧岩浆岩(耿全如等, 2005;Zhu et al., 2008; Kang et al., 2014; 黄丰等, 2015),其中的玄武岩同样具有较低的TiO_2和Nb含量(TiO_2多数小于1%,Nb多数小于3×10^{-6};Kang et al., 2014; 黄丰等, 2015)。但汤白辉绿岩脉与这些弧岩浆岩相比具有较高的TiO_2和Nb含量(TiO_2=0.97%~1.02%,4.01×10^{-6}~4.54×10^{-6})。在微量元素原始地幔标准化蛛网图解中(图7b),与安第斯山弧和马里亚纳弧玄武岩相比,其Nb、Ta和Ti亏损较弱。更重要的是汤白辉绿岩脉具有比典型弧岩浆岩更高的Zr含量,典型弧岩浆岩一般小于50×10^{-6}(Xu et al., 2008),同时区域上叶巴组和桑日群中的玄武岩Zr含量普遍为60×10^{-6}~80×10^{-6}(Zhu et al., 2008; Kang et al., 2014; 黄丰等, 2015),而汤白辉绿岩脉Zr含量为98.8×10^{-6}~100×10^{-6},远高于典型弧岩浆岩甚至区域上叶巴组和桑日群的玄武岩,在Zr−Zr/Y玄武岩构造环境判别图解中(图8a),汤白辉绿岩脉落在了板内玄武岩区域,这明显不同于弧玄武岩,显示出板内伸展背景下玄武岩地球化学属性;在2×Nb−Zr/4−Y玄武岩构造环境判别图解中(图8b),汤白辉绿岩脉同样显示出板内玄武岩地球化学属性。在研究区北侧和西侧,一些学者同样发现过地球化学性质与此极其类似的基性岩浆岩,赵志丹等(2011)、贾黎黎等(2013)和Huang et al.(2017)分别对当雄辉长岩

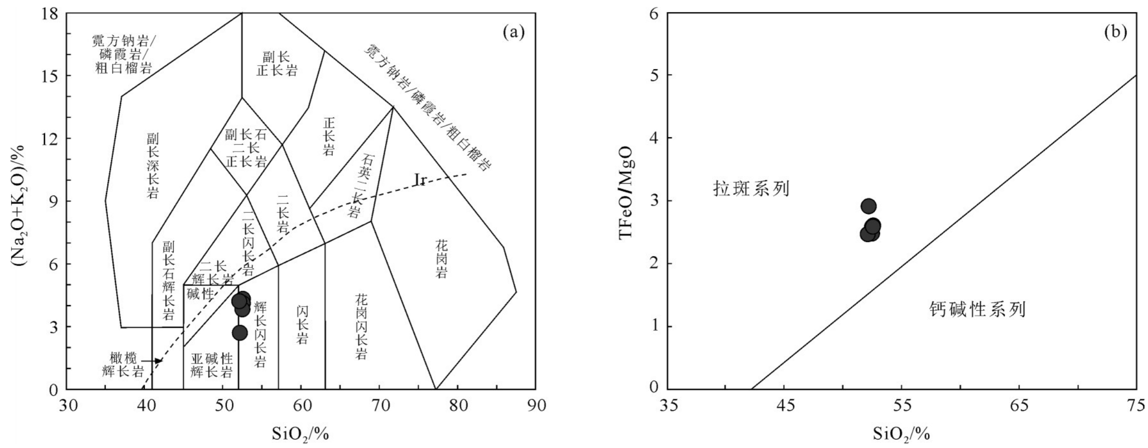

图6 汤白辉绿岩脉TAS（a）和SiO_2−TFeO/MgO（b）图解
（a据Middlemost, 1994; b据 Miyashiro, 1974）
Fig. 6 TAS (a) and K_2O−TFeO/MgO (b) diagrams of the Tangbai diabase dikes
（a after Middlemost, 1994; b after Miyashiro, 1974）

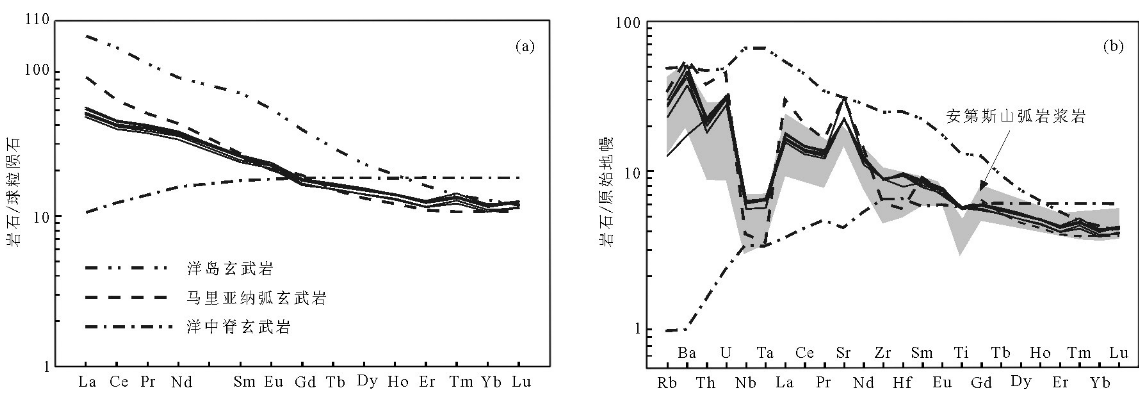

图7 汤白辉绿岩脉稀土元素球粒陨石标准化配分图（a）和微量元素原始地幔标准化蛛网图（b）
(洋岛玄武岩、洋中脊玄武岩、球粒陨石值和原始地幔值据Sun and Mcdonough, 1989; 马里亚纳弧玄武岩据Peate and Pearce, 1998;
安第斯山弧岩浆岩据Xu et al., 2008)
Fig.7 Chondrite−normalized REE distribution patterns (a) and primitive mantle−normalized trace element spidergrams (b) of the Tangbai diabase dikes
(OIB, N−MORB, chondrite and primitive mantle data after Sun and McDonough, 1989; data of Mariana arc basalts after Peate and Pearce, 1998; data of Andean arc basalts after Xu et al., 2008)

（54 Ma）、林周盆地基性岩脉（52.5 Ma）和达孜一带的镁铁质岩脉（57 Ma）进行研究后，发现这些基性岩浆岩同样具有较高的Zr含量和较高的Zr/Y比值（图8a），当雄辉长岩个别岩体Zr含量达到173×10^{-6}（赵志丹等, 2011），因此这些学者一致认为这些基性岩浆岩具有板内玄武岩地球化学属性，侵位于局部应力释放的伸展构造背景下，类似于板内伸展背景下玄武岩。

5.3 岩石成因

5.3.1 混染作用

微量元素原始地幔标准化蛛网图显示出的强烈Ta、Nb亏损，可能是俯冲作用引起的交代或陆壳混染作用所致（Pearce and Cann, 1973；Green et al., 2000），这两种形式的混染过程都可以产生相同的结果，即地壳物质加入到岩浆中，不同之处在于二者混染的位置不同，俯冲相关的交代作用发生在岩浆源区，而陆壳混染发生岩浆侵位上升的过程中（Smithes et al., 2004）。

一般认为，如果岩浆在上升侵位过程中受到了地壳物质混染，岩浆岩的La/Sm比值将会明显增大，一般会大于5（Lassiter and Depaoolo, 1997）。本文研究的汤白辉绿岩脉的La/Sm比值变化范围为

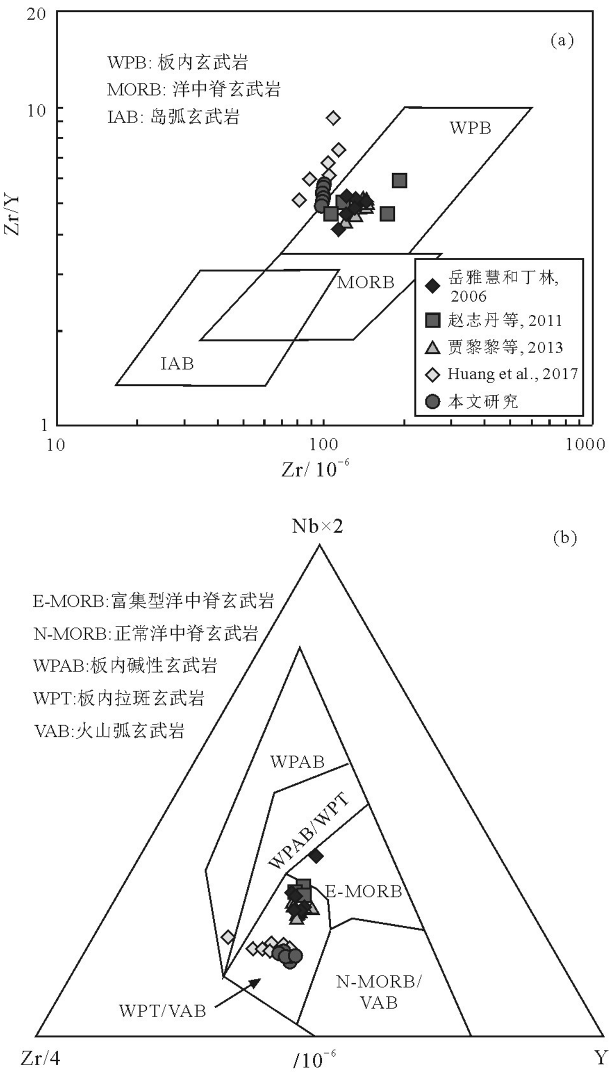

图8 汤白辉绿岩脉微量元素构造环境判别图
(a据Pearce and Norry, 1979; b据Meschede, 1986)
Fig.8 Trace element discrimination diagram of the tectonic setting of the Tangbai diabase dikes
(a after Pearce and Norry, 1979; b after Meschede, 1986)

2.97~3.26,平均值为3.11,明显小于5,在La/Sm−La/Nb图解中(图9a),辉绿岩脉的La/Nb值变化较小(2.50~3.10),且与La/Sm比值没有明显的正相关关系,说明岩浆在上升侵位过程中受地壳物质混染的可能性较小。在MgO−Nb/La图解中(图9b),Nb/La比值并不随着MgO的含量增加而增加,同样说明岩浆上升侵位的过程中未受到地壳物质的明显混染。此外汤白辉绿岩脉样品具有较高的Nb/Ta比值(平均值为16.8)、Zr/Hf比值(平均值35)和Lu/Yb比值(平均值0.16),与洋中脊玄武岩值接近(Nb/Ta=17.7,Zr/Hf=36.2,Lu/Yb=0.15,据Sun and McDonough, 1989),高于大陆地壳值(Nb/Ta=11,Zr/Hf=33,Lu/Yb=0.14,据Taylor and Mclennan, 1995)。进一步指示汤白辉绿岩脉没有受到明显的地壳混染。岳雅慧和丁林(2006)对林周盆地基性岩脉(52.5 Ma)进行Sr、O同位素研究后同样认为这些基性岩脉在上升过程中未受到地壳物质的混染。综上所述,可以排除汤白辉绿岩脉在上升侵位过程中受到了地壳物质的混染。那么Ta、Nb的亏损可能继承了岩浆源区的性质,说明混染作用主要发生在岩浆源区。在源区引起混染作用的形式主要有两种,一种是俯冲板片释放流体交代地幔橄榄岩,另一种熔体交代地幔橄榄岩,下面将要讨论究竟是板片释放的流体还是熔体对岩浆源区进行交代。

微量元素在含水流体中的活动性研究表明,稀土元素(如Yb)以及高场强元素(如Th、Nb、Ta和Zr等)均为不活动或活动性较弱的元素,而大离子亲石元素(如Rb、Sr、Ba和U等)活动性较强。在板块俯冲带,Th在大洋沉积物中具有较高的含量(Othman et al., 1989; Plank and Langmuir, 1998),而Ba、Sr活动性较强,容易进入俯冲板片所释放的流体中(Sano et al., 2001),那么如果是熔体交代地幔橄榄岩,岩石中Th的含量会明显增大,如果是流体交代地幔橄榄岩,Ba、Sr在岩石中的含量也会明显增大。汤白辉绿岩脉具有较高的Ba/Th比值(图10a),暗示俯冲带释放的流体对源区岩浆具有显著贡献。在Th/Nb−Sr/Ta元素变异图解中(图10b),辉绿岩脉具有相对稳定的Th/Nb比值(0.38~0.43),变化较大的Sr/Ta比值(1731~2444),同样暗示俯冲带的流体对源区岩浆具有显著贡献。在Th/Yb−Ba/La和Nb/Zr−Th/Zr(图10c、d)图解中,均显示岩浆源区受到了俯冲板片释放的流体的明显交代作用,这与新特提斯洋在晚三叠世—侏罗纪或更早开始俯冲的地质事实相吻合(莫宣学等, 2005; Chu et al., 2006, 2011; Guo et al., 2013; Lang et al., 2014; Meng et al., 2016),因此引起Nb、Ta相对亏损的主要原因是早期俯冲板片在俯冲的过程中所释放的流体交代岩浆源区。

5.3.2 *岩石源区*

玄武质岩浆通常起源于岩石圈地幔或软流圈地幔,起源于岩石圈地幔的岩浆形成的岩石相对于

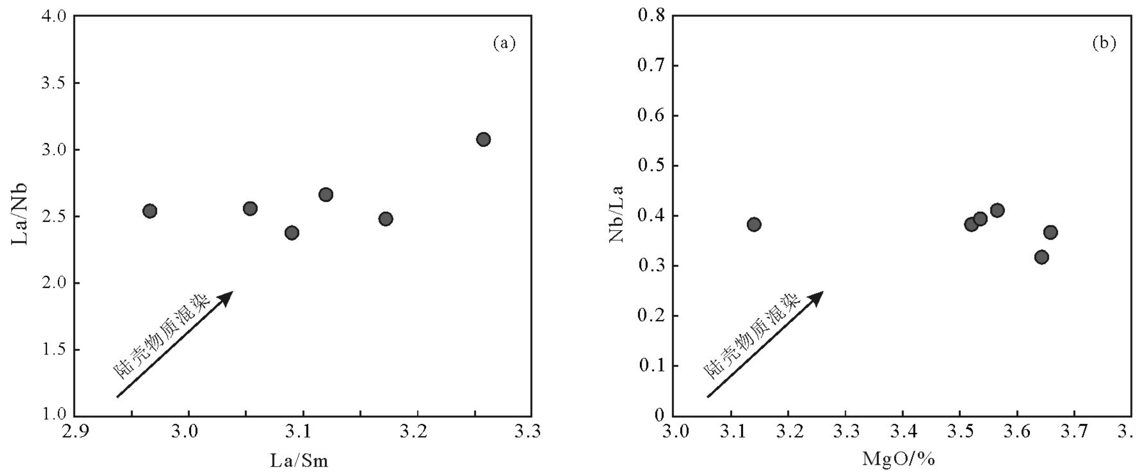

图9 汤白辉绿岩脉La/Sm−La/Nb 7(a)和MgO−Nb/La(b)图解

(a据Macdonald et al., 2001; b据Tang et al., 2013)

Fig. 9 La/Sm−La/Nb (a) and MgO−Nb/La (b) diagrams of the Tangbai diabase dikes

a after Macdonald et al., 2001; b after Tang et al., 2013

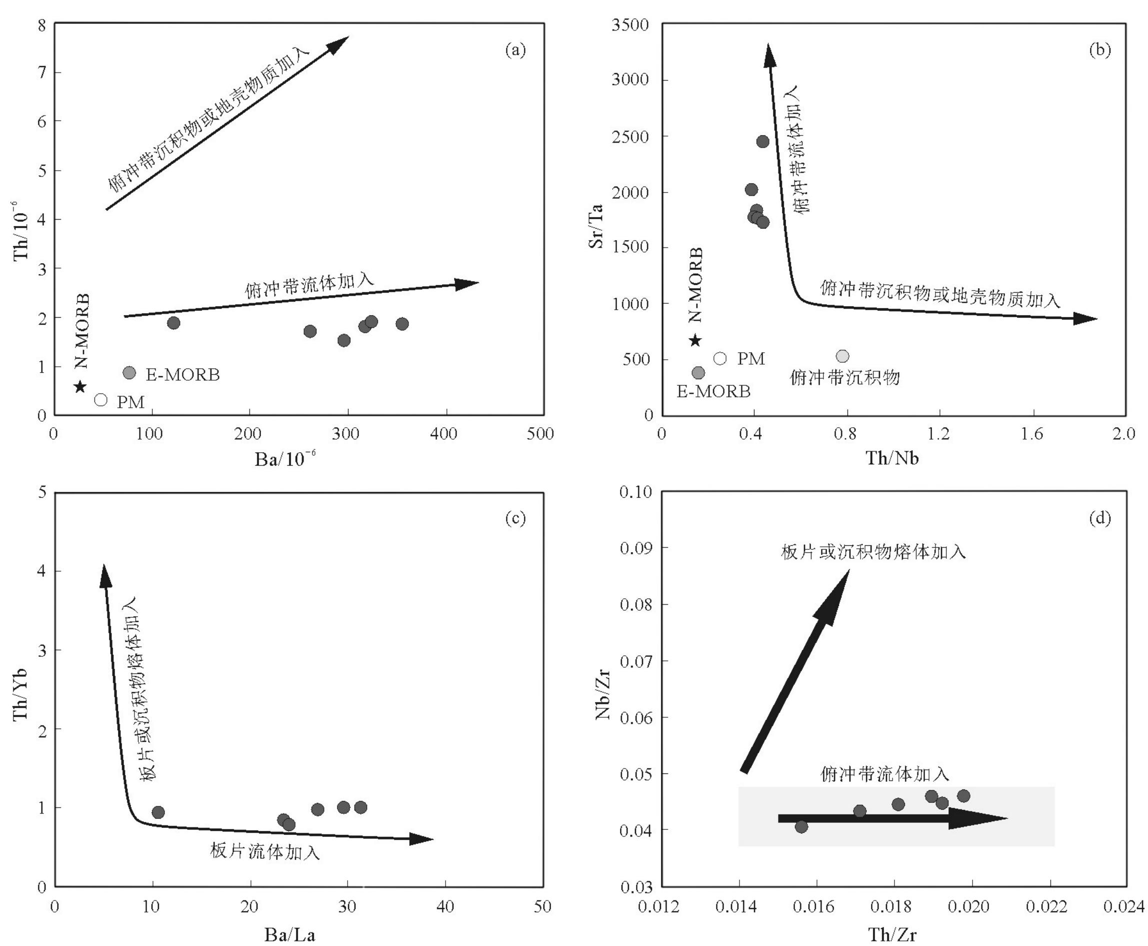

图10 汤白辉绿岩Ba−Th(a)、Th/Nb−Sr/Ta(b)、Ba/La−Th/Yb(c)和Th/Zr−Nb/Zr(d)元素变异图解

(a和b据安芳等, 2014; c据Woodhead et al., 2001; d据Zhao and Zhou, 2007)

Fig.10 Trace elements variation diagrams of Ba−Th (a), Th/Nb−Sr/Ta (b), Ba/La−Th/Yb (c) and Th/Zr−Nb/Zr (d) of the Tangbai diabase dikes

(a and b after An Fang et al., 2014; c after Woodhead et al., 2001; d after Zhao and Zhou, 2007)

原始地幔通常富集轻稀土元素和大离子亲石元素，亏损高场强元素；而起源于软流圈地幔的岩浆形成的岩石通常富集大离子亲石元素（LILE）和高场强元素（HFSE）（Sklyarov et al., 2003; Zhao and Zhou, 2007; 刘彬等, 2013）；汤白辉绿岩脉明显富集轻稀土元素（LREE）和大离子亲石元素（LILE），亏损高场强元素（HFSE）（图7a、b），说明汤白辉绿岩脉可能起源于部分熔融的岩石圈富集地幔。然而前文已经提到汤白辉绿岩脉、当雄南部的辉长岩、达孜铁镁质岩脉及林周盆地的基性岩脉具有高于典型岛弧岩浆岩、区域上叶巴组和桑日岩群中玄武岩的TiO_2、Zr和Nb含量，说明岩浆源区可能有更深的软流圈地幔物质的加入（赵志丹等, 2011; 贾黎黎等, 2013; Huang et al., 2017）。此外汤白辉绿岩脉不均一的Hf同位素特征（$\varepsilon_{Hf}(t)$= −3.9~8.9，图5）也显示出其源区经历了富集地幔和亏损地幔的混合作用。在研究区的西部，达孜铁镁质岩脉变化范围较大锆石$\varepsilon_{Hf}(t)$值（$\varepsilon_{Hf}(t)$= −5.5~10.1，图5；Huang et al., 2017）进一步支持了拉萨地体南缘早始新世基性岩浆岩源区具有亏损地幔和富集地幔双重特征。因此笔者认为汤白辉绿岩脉的源区除起源于部分熔融的岩石圈富集地幔外，同时还有深部软流圈亏损地幔物质加入。根据McKenzie and Bickle（1988）的研究表明，干的软流圈部分熔融的条件仅当岩石圈是非常的薄的时候才能发生（< 70~80 km），考虑到当时拉萨地体地壳并未明显加厚（Mo et al., 2007），以及汤白辉绿岩脉、林周盆地基性岩脉和达孜铁镁质岩脉，这些类似板内伸展背景下的基性岩脉存在同样暗示当时地壳是非常薄的并处于拉张构造背景，表明软流圈地幔上涌发生减压部分熔融是可能存在的。

重稀土元素Yb对石榴子石是强相容的，而对尖晶石强不相容的（Arth and Barker, 1976; Carlos, 1977; Xu et al., 2005），Xu et al.（2005）研究表明La/Yb和Sm/Yb能够在相对深的石榴子石二辉橄榄岩稳定区发生部分熔融时呈现明显分异；相反，在相对浅的尖晶石二辉橄榄岩稳定区La/Yb呈现弱分异，Sm/Yb不分异（图11a），因此岩浆岩的La/Yb和Sm/Yb比值能够判别岩浆源区石榴石和尖晶石含量变化及岩浆起源深度，汤白辉绿岩脉均落在石榴子石二辉橄榄岩熔融曲线上（图11a），且源区部分熔融的程度约20%。在La/Yb−Dy/Yb图解中（图11b），汤白辉绿岩脉落在石榴子石二辉橄榄岩熔融曲线附近，其源区熔融的程度约20%，进一步说明了岩浆源区及源区熔融的程度。McKenzie and O'Nions（1991）和Robinson and Wood（1998）的研究成果表明，尖晶石二辉橄榄岩稳定区与石榴子石二辉橄榄岩稳定区的过渡区间对应的深度为75~80 km，那么本文研究的辉绿岩脉落在了石榴子石二辉橄榄岩稳定区，说明岩浆起源的深度大于80 km。

5.4 成岩模式及构造意义

汤白辉绿岩脉成岩模式应合理解释以下几个问题：(1)汤白辉绿岩脉具有弧玄武岩浆和板内玄武岩浆的双重地球化学属性；(2)岩浆在上升侵位的过程中未遭受地壳物质混染；(3)岩浆源区有来

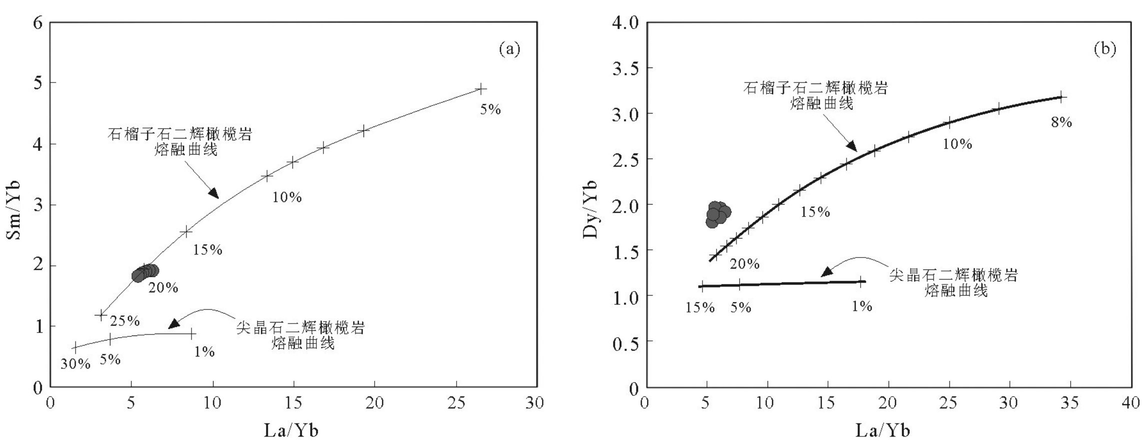

图11 汤白辉绿岩脉La/Yb−Sm/Yb(a)和La/Yb−Dy/Yb(b)图解
（a据Xu et al., 2005; b据Bogaard and Wörner, 2003）
Fig. 11 La/Yb−Sm/Yb (a) and La/Yb−Dy/Yb (b) diagram of the Tangbai diabase dikes
(a after Xu et al., 2005; b after Bogaard and Wörner, 2003)

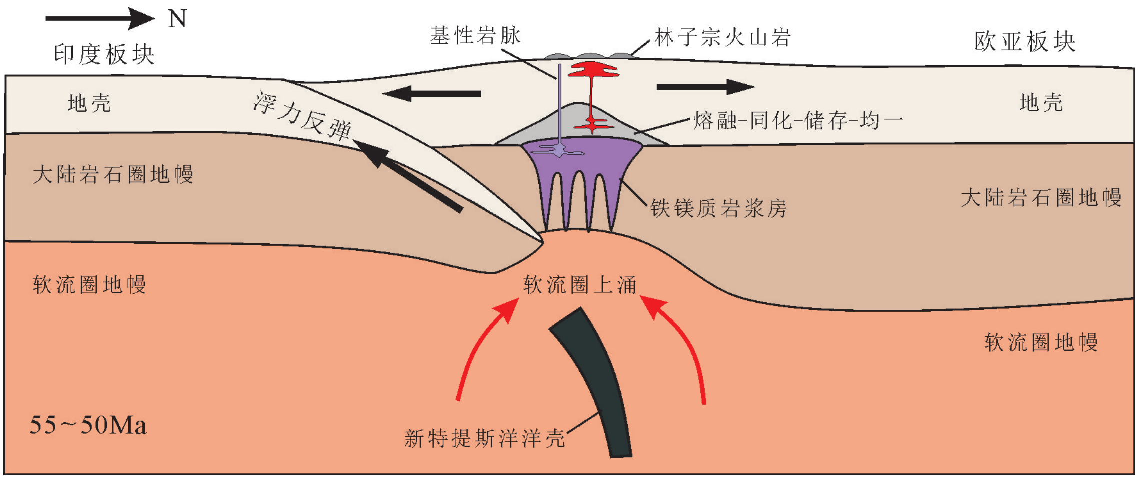

图12 汤白辉绿岩脉成岩模式图(据岳雅慧和丁林, 2006修改)
Fig. 12 Petrogenetic model for the Tangbai diabase dikes (modified from Yue Yahui and Ding Lin, 2006)

源于较深的软流圈亏损地幔物质的部分熔融。结合这一时期岩浆岩的时空分布、岩浆源区性质、岩浆侵位机制和前人的研究成果(Ding et al., 2003; Chung et al., 2005; 岳雅慧和丁林, 2006; Xu et al., 2008; Lee et al., 2009;赵志丹等, 2011; 贾黎黎等, 2013; 董铭淳等, 2015; Tian et al., 2017; Huang et al., 2017),可以通过板片断离的模型来解释汤白辉绿岩脉形成的动力学机制(图12)。

在板片断离之前,俯冲板片前缘的新特提斯洋片由于脱水,密度增大,使得前缘洋片发生陡深俯冲——“板片回转作用”(Chung et al., 2005; 岳雅慧和丁林, 2006),俯冲板片前缘的密度较大的洋壳拖拽随后密度较小的印度大陆向北漂移,使其到达海沟位置向欧亚大陆下俯冲,由于大陆岩石圈的密度较深部地幔小,使其受到一个与下部拖拽力相反的浮力,便在大陆地壳和俯冲大洋板片之间产生一个很强的拉张力(Davies and von Blanckenburg, 1995),随着拉张力逐渐积累,当超过板片薄弱地带的最大承受能力时,便使大洋板片与印度大陆岩石圈发生断裂(图12),这时软流圈地幔沿着断裂位置上涌,提供了物质和热量,使受早期俯冲流体交代的岩石圈地幔发生部分熔融,并与之混合一起上侵,因此汤白辉绿岩脉显示出起源于岩石圈富集地幔和软流圈亏损地幔的双重特征。另一方面由于俯冲板片前缘洋壳断离脱落,拉力突然释放,在浮力的作用下印度大陆发生短暂回撤,同时拖拽上覆的欧亚大陆南缘,产生一个局部伸展地带(图12),因此汤白辉绿岩脉在上升的过程中没有明显受到地壳物质的混染,显示出板内玄武岩浆的地球化学属性。

在造山旋回中,洋壳俯冲结束至陆陆碰撞的开始标志一个重大地质演化不连续事件,因此一直以来备受关注,关于印度板块与欧亚大陆碰撞的起始时间不同学者提出不同的观点,一些学者认为早于55 Ma(Jaeger et al., 1989; Liu and Einsele, 1994; Yin and Harrison, 2000; Leech et al., 2005; 莫宣学等, 2003, 2007; Xu et al., 2008; 黄宝春等, 2010),另一些则认为晚于55 Ma(Searle et al., 1987; Dewey et al., 1989; Aitchison, 2007)。本文报道的汤白辉绿岩脉年龄为54 Ma,在中部拉萨地体中段赵志丹等(2011)和贾黎黎等(2013)分别报道过当雄南部约54 Ma辉长岩和林周盆地约52.5 Ma的基性岩脉,这些基性岩浆岩均显示板内岩浆岩的特征,被认为是板片断离的产物。如果这些基性岩浆岩的年龄和地球化学特征是可靠的,在此可以试图约束印度板块与欧亚大陆碰撞的起始时间。

板片的断离通常发生于陆陆碰撞的早期阶段(Davies and Von Blanckenburg, 1995; Wong et al., 1997),所以印度板块与欧亚大陆碰撞的起始时间一定是早于本文报道的辉绿岩脉年龄(54 Ma),尽管在大陆碰撞发生后的板片断离时间取决于诸多因素(Wong et al., 1997; Gerya et al., 2004),但最近基于三维数值模拟实验研究表明,根据俯冲洋壳的性质不同,板片的断离时间一般发生在陆陆碰撞之后10~25 Ma(Van Hunen and Allen, 2011)。同时该

模型得到的广泛运用,在阿拉伯—欧亚碰撞带,约35 Ma时构造、岩浆和地层发生改变,被认为是陆陆碰撞的起始时间,在20 Ma时,这种变化进一步加剧被认为是板片断离的结果(Van Hunen and Allen., 2011)。在拉萨地体中段本文和前人(赵志丹等, 2011; 贾黎黎等, 2013; Huang et al., 2017)报道的具有板内性质的基性岩浆岩与区域上岩浆岩爆发高峰的时间相近(52 Ma, Yin and Harrison, 2000; Flower et al., 2001; 莫宣学等, 2003; He et al., 2007; Mo et al., 2007; Lee et al., 2009),因此将板片断离的时间确定为54~52 Ma是合理的。基于Van Hunen and Allen(2011)的地质模型和区域地质事件(莫宣学等, 2003, 2007; Mo et al., 2007),笔者认为印度板块与欧亚大陆碰撞起始的时间应该为65 Ma或者更早。

6 结 论

(1)汤白辉绿岩脉LA−ICP−MS锆石U−Pb年龄为(54±1) Ma,形成时代为早始新世,与区域上林子宗火山岩爆发峰期时间接近(52 Ma)。

(2)汤白辉绿岩脉微量元素及锆石Hf同位素特征显示岩浆源区除来自于受早期俯冲板片释放的流体交代的岩石圈富集地幔外,同时有更深部的软流圈亏损地幔的物质加入,岩浆起源于二辉橄榄岩的部分熔融,起源深度大于80 km。

(3)汤白辉绿岩脉形成与新特提斯洋板片断离有关,侵位于印度大陆瞬间回撤伸展的构造环境中;上升侵位的过程中未受到地壳的混染,显示出板内玄武岩地球化学属性。

(4)汤白辉绿岩脉成岩动力学机制为新特提斯洋板片断离,其断离的时间为54~52 Ma,为印度板块与欧亚大陆碰撞的起始时间提供约束,认为两者开始碰撞的时间为65 Ma或者更早。

References

Amelin Y, Halliday A N, Lee D C. 2000. Early−middle archaean crustal evolution deduced from Lu−Hf and U−Pb isotopic studies of single zircon grains[J]. Geochimica et Cosmochimica Acta, 64 (24): 4205−4225.

Aitchison J C, Ali J R, Davis A M. 2007. When and where did India and Asia collide?[J]. Journal of Geophysical Research Solid Earth, 112(B5): 51−70.

Arth J G, Barker F. 1976. Rare−earth partitioning between hornblende and dacitic liquid and implications for the genesis of trondhjemitic−tonalitic magmas[J]. Geology, 4(9): 534.

An Fang, Zhu Yongfeng, Wei Shaoni, Lai Shacong. 2014. Geochronology and geochemistry of Shizishan sub−volcanic rocks in Jingxi− Yelmand gold deposit, Northwest Tianshan: Its petrogenesis and implications to tectonics and Au−mineralization[J]. Acta Petrologica Sinica, 30(6): 1545−1557 (in Chinese with English abstract).

Boekhout F, Spikings R, Sempere T, Chiaradia M, Ulianov A, Schaltegger U. 2012. Mesozoic arc magmatism along the southern Peruvian margin during Gondwana breakup and dispersal[J]. Lithos, s146−147(8): 48−64.

Bogaard P J F, Wörner G. 2003. Petrogenesis of Basanitic to Tholeiitic Volcanic Rocks from the Miocene Vogelsberg, Central Germany[J]. Journal of Petrology, 44(3): 569−602.

Carlos A R. 1977. Geochemistry of the tonalitic and granitic rocks of the Nova Scotia southern plutons[J]. Geochimica et Cosmochimica Acta, 41(1): 1−13.

Chu M F, Chung S L, O'Reilly S Y, Pearson N J, Wu F Y, Li X H, Liu D Y, Ji j Q, Chu C H, Lee H Y. 2011. India's hidden inputs to Tibetan orogeny revealed by Hf isotopes of Transhimalayan zircons and host rocks[J]. Earth & Planetary Science Letters, 307 (3): 479−486.

Chu M F, Chung S L, Song B, O'Reilly S Y, Pearson N J, Ji J Q, Wen D J. 2006. Zircon U− Pb and Hf isotope constraints on the Mesozoic tectonics and crustal evolution of southern Tibet[J]. Geology, 34(9): 745.

Chung S L, Chu M F, Zhang Y Q, Xie Y W, Lo C H, Lee T Y, Lan C Y, Li X H, Zhang Q, Wang Y Z. 2005. Tibetan tectonic evolution inferred from spatial and temporal variations in post− collisional magmatism[J]. Earth−Science Reviews, 68(3/4): 173−196.

Chung S L, Liu D Y, Ji J Q, Chu M F, Lee H Y, Wen D J, Lo C H, Lee T Y, Qian Q, Zhang Q. 2003. Adakites from continental collision zones: Melting of thickened lower crust beneath southern Tibet[J]. Geology, 31(11): 1021−1024.

Cui X Z, Jiang X S, Wang J, Wang X C, Zhuo J W, Deng Q, Liao S Y, Wu H, Jiang Z F, Wei Y A. 2015. Mid− Neoproterozoic diabase dykes from Xide in the western Yangtze Block, South China: New evidence for continental rifting related to the breakup of Rodinia supercontinent[J]. Precambrian Research, 268: 339−356.

Davies J H, Von Blanckenburg F. 1995. Slab breakoff: A model of lithosphere detachment and its test in the magmatism and deformation of collisional orogens[J]. Earth & Planetary Science Letters, 129(1/4): 85−102.

Dewey J F, Cande S C, Pitman W C I. 1989. Tectonic evolution of the India/Eurasia Collision Zone[J]. Eclogae Geologicae Helvetiae, 82 (3): 717−734.

Ding L, Kapp P, Zhong D L, Deng W M. 2003. Cenozoic Volcanism in Tibet: Evidence for a Transition from Oceanic to Continental Subduction[J]. Journal of Petrology, 44(10): 1833−1865.

Dong G C, Mo X X, Zhao Z D, Guo T Y, Wang L L, Chen T. 2005.

Geochronologic constraints on the magmatic underplating of the gangdisê belt in the india−eurasia collision: evidence of SHRIMP II zircon U−Pb dating[J]. Acta Geologica Sinica, 79(6): 787−794.

Dong Guochen, Mo Xuanxue, Zhao Zhidan, Zhu Dicheng, Song Yuntao, Wang Lei. 2008. Gabbros from southern gangdese: Implication for mass exchange between mantle and crust[J]. Acta Petrologica Sinica, 24(2): 203− 210 (in Chinese with English abstract).

Dong Mingchun, Zhao Zhidan, Zhu Dicheng, Liu Dong, Dong Guochen, Mo Xuanxue, Hu Zhaochu, Liu Yongsheng, Zou Zihao. 2015. Geochronology, geochemistry, and petrogenesis of the intermediate and acid dykes in Linzhou Basin, southern Tibet[J]. Acta Petrologica Sinica, 31(5): 1268− 1284 (in Chinese with English abstract).

Dong X, Zhang Z M, Santosh M. 2010. Zircon U−Pb Chronology of the Nyingtri Group, Southern Lhasa Terrane, Tibetan Plateau: Implications for Grenvillian and Pan− African Provenance and Mesozoic− Cenozoic Metamorphism[J]. The Journal of Geology, 118(6): 677−690.

Ernst R E, Wingate M T D, Buchan K L, Li Z X. 2008. Global record of 1600− 700 Malarge igneous provinces (LIPs): implications for the reconstruction of the pro−posed Nuna (Columbia) and Rodinia supercontinents[J]. Precambrian Research, 160: 159−178.

Flower M F J, Russo R M, Tamaki K, Hoang N. 2001. Mantle contamination and the Izu− Bonin− Mariana (IBM) 'high− tide mark': evidence for mantle extrusion caused by Tethyan closure[J]. Tectonophysics, 333(1/2): 9−34.

Gao Y F, Yang Z S, Santosh M, Hou Z Q, Wei R H, Tian S H. 2010. Adakitic rocks from slab melt− modified mantle sources in the continental collision zone of southern Tibet[J]. Lithos, 119(3/4): 651−663.

Gao Yongfeng, Hou Zengqian, Wei Ruihua, Meng Xiangjing, Hu Huabin. 2006. The geochemistry and Sr− Nd− Pb isotopes of basaltic subvolcanics from the gangdese: Contraints on depleted mantle source post− collisional volcanisms in the Tibetan plateau[J]. Acta Petrologica Sinica, 22(3): 547− 557 (in Chinese with English abstract).

Geng Quanru, Pan Guitang, Jin Zhenmin, Wang Liquan, Zhu Dichen, Liao Zhongli. 2005. Geochemistry and Genesis of the Yeba Volcanic Rocks in the Gangdise Magmatic Arc, Tibet[J]. Earth Science−Journal of China University of Geosciences, 30(6): 747−760 (in Chinese with English abstract).

Gerya T V, Yuen D A, Maresch W V. 2004. Thermomechanical modeling of slab detachment[J]. Earth & Planetary Science Letters, 226(1/2): 101−116.

Gladkochub D P, Wingate T M D, Pisarevsky S A, Donskaya T V, Mazukabzov A M, Ponomarchuk V A, Stanevich A M. 2006. Mafic intrusions in southwestern Siberia and implications for a Neoproterozoic connection with Laurentia[J]. Precambrian Research, 147: 260−278.

Green M G, Sylvester P J, Buick R. 2000. Growth and recycling of early Archaean continental crust: Geochemical evidence from the Coonterunah and Warrawoona Groups, Pilbara Craton, Australia[J]. Tectonophysics, 322(1/2): 69−88.

Guo L H, Liu Y L, Liu S W, Cawood P A, Wang Z H, Liu H F. 2013. Petrogenesis of Early to Middle Jurassic granitoid rocks from the Gangdese belt, Southern Tibet: Implications for early history of the Neo−Tethys[J]. Lithos, 179(5): 320−333.

Guynn J H, Kapp P, Pullen A, Heizier M, Gehrels G, Ding L. 2006. Tibetan basement rocks near Amdo reveal "missing" Mesozoic tectonism along the Bangong suture, central Tibet[J]. Geology, 34 (6): 505−508.

He S D, Kapp P, Decelles P G, Gehrels G E, Heizler M. 2007. Cretaceous−Tertiary geology of the Gangdese Arc in the Linzhou area, southern Tibet[J]. Tectonophysics, 433(1/4): 15−37.

Hoek J D, Seitz H M. 1995. Continental mafic dykes warms as tectonic indicators: an example from the Vestfold Hills, East Antarctica[J]. Precambrian Research, 75: 121−139.

Holm P M, Heaman L M, Pedersen L E. 2006. Baddeleyite and zircon U−Pb ages from the Kaerven area, Kangerlussuaq: implications for timing of Paleogene continental breakup in the North Atlantic[J]. Lithos, 92: 238−250.

Hoskin P W O, Black L P. 2000. Metamorphic zircon formation by solid−state recrystallization of protolith igneous zircon[J]. Journal of Metamorphic Geology, 18(4): 423−439.

Hou Kejun, Li Yanhe, Zou Tianren, Qu Xiaoming, Shi Yuruo, Xie Guiqing. 2007. Laser ablation− MC− ICP− MS technique for Hf isotope microanalysis of zircon and its geological appfications[J]. Acta Petrologlca Sinica, 23(10): 2595− 2604 (in Chinese with English abstract).

Hou G T, Santosh M, Qian X L, Lister G S, Li J H. 2008. Tectonic constraints on 1.3− 1.2 Ga final breakup of Columbia supercontinent from a giant radiating dykes warm[J]. Gondwana Research, 14: 561−566.

Hou Z Q, Duan L F, Lu Y J, Zheng Y C, Zhu D C, Yang Z M, Yang Z S, Wang B D, Pei Y R, Zhao Z D, McCuaig C T. 2015. Lithospheric Architecture of the Lhasa Terrane and Its Control on Ore Deposits in the Himalayan− Tibetan Orogen[J]. Economic Geology, 110: 1541−1575.

Hou Z Q, Gao Y F, Qu X M, Rui Z Y, Mo X X. 2004. Origin of adakitic intrusives generated during mid− miocene east− west extension in southern Tibet[J]. Earth & Planetary Science Letters, 220(1/2): 139−155.

Huang Baochun, Chen Junshan, Yi Zhiyu. 2010. Paleomagnetic discussion of when and where India and Asia initially collided[J]. Chninese journal of Geophysics, 53(9): 2045− 2058 (in Chinese with English abstract).

Huang Feng, Xu Jifeng, Chen Jianlin, Kang Zhiqiang, Dong Yanhui. 2015. Early Jurassic volcanic rocks from the Yeba Formation and Sangri Group: Products of continental marginal arc and intra−oceanic arc during the subduction of Neo−Tethys Ocean?[J]. Acta Petrologica Sinica, 31(7): 2089− 2100 (in Chinese with English abstract).

Huang F, Xu J H, Zeng Y C, Chen J L, Wang B D,Yu H X, Chen L, Huang W L, Tan R Y. 2017. Slab Breakoff of the Neo−ethys Ocean in the Lhasa Terrane Inferred From Contemporaneous Melting of the Mantle and Crust[J]. Geochemistry, Geophysics, Geosystems, DOI: 10.1002/2017GC007039.

Jaeger J J, Courtillot V, Tapponnier P. 1989. Paleontological view of the ages of the Deccan Traps, the Cretaceous/Tertiary boundary, and the India−Asia collision[J]. Geology, 17(4): 316.

Ji W Q, Wu F Y, Chung S L, Li J X, Liu C Z. 2009a. Zircon U−Pb geochronology and Hf isotopic constraints on petrogenesis of the Gangdese batholith, southern Tibet[J]. Chemical Geology, 262(3): 229−245.

Ji W Q, Wu F Y, Liu C Z, Chung S L. 2009b. Geochronology and petrogenesis of granitic rocks in Gangdese batholith, southern Tibet[J]. Science in China (Series D): Earth Sciences, 52(9): 1240−1261.

Jia Lili, Wang Qing, Zhu Dicheng, Chen Yue, Wu Xingyuan, Liu Shengao, Zheng Jianping, Zhao Tianpei. 2013. Rethinking the geodynamical implications of the basic rocks from Linzhou Basin, Tibet[J]. Acta Petrologica Sinica, 29(11): 3671−3680 (in Chinese with English abstract).

Kang Z Q, Xu J F, Wilde S A, Feng Z H, Chen J L, Wang B D, Fu W C, Pan H B. 2014. Geochronology and geochemistry of the Sangri Group Volcanic Rocks, Southern Lhasa Terrane: Implications for the early subduction history of the Neo− Tethys and Gangdese Magmatic Arc[J]. Lithos, 200(1): 157−168.

Lang X H, Tang J X, Li Z J, Huang Y, Ding F, Yang H H, Xie F W, Zhang L, Wang Q, Zhou Y. 2014. U− Pb and Re− Os geochronological evidence for the Jurassic porphyry metallogenic event of the Xiongcun district in the Gangdese porphyry copper belt, southern Tibet, PRC[J]. Journal of Asian Earth Sciences, 79 (2): 608−622.

Lassiter J C, Depaoolo D J. 1997. Plume/lithosphere interaction in the generation of continental and oceanic flood basalts: Chemical and isotopic constraints. In large igneous provinces: Continental, oceanic, and planetary flood volcanism[C]//Geophysical Monography 100, Am Geophys Union, 335−355.

Lee H Y, Chung S L, Ji J Q, Qian Q, Gallet S, Lo C H, Lee T Y, Zhang Q. 2012. Geochemical and Sr− Nd isotopic constraints on the genesis of the Cenozoic Linzizong volcanic successions, southern Tibet[J]. Journal of Asian Earth Sciences, 53(2): 96−114.

Lee H Y, Chung S L, Lo C H, Ji J Q, Lee T Y, Qian Q, Zhang Q. 2009. Eocene Neotethyan slab breakoff in southern Tibet inferred from the Linzizong volcanic record[J]. Tectonophysics, 477(1/2): 20−35.

Leech M L, Singh S, Jain A K, Klemperer S L, Manickavasagam R M. 2005. The onset of India− Asia continental collision: Early, steep subduction required by the timing of UHP metamorphism in the western Himalaya[J]. Earth & Planetary Science Letters, 234(1−2): 83−97.

Liu Bin, Ma Changqian, Jiang Hongan, Guo Pan, Zhang Jinyang, Xiong Fuhao. 2013. Early Paleozoic tectonic transition from ocean subduction to collisional orogeny in the Eastern Kunlun region: Evidence from Huxiaoqin mafic rocks[J]. Acta Petrologica Sinica, 29(6): 2093−2106 (in Chinese with English abstract).

Liu G, Einsele G. 1994. Sedimentary history of the Tethyan basin in the Tibetan Himalayas[J]. Geologische Rundschau, 83(1): 32−61.

Liu Liwen, Li Jianfeng, Xiabin, Qiu Liangbin, Huang Qiangtai. 2012. Chronology and geochemical characteristics of Namuru island arc volcanics in Tibet[J]. Bulletin of Mineralogy Petrology and Geochemistry, 31(2): 114−120 (in Chinese with English abstract).

Macdonald R, Rogers N W, Fitton J G, Black S, Smith M. 2001. Plume−Lithosphere Interactions in the Generation of the Basalts of the Kenya Rift, East Africa[J]. Journal of Petrology, 42(5): 877−900.

Martin H, Smithies R H, Rapp R, Moyen J F, Champion D. 2005. An overview of adakite, tonalite− trondhjemite− granodiorite (TTG), and sanukitoid: relationships and some implications for crustal evolution[J]. Lithos, 79(1/2): 1−24.

Mckenzie D, Bickle M J. 1988. The Volume and Composition of Melt Generated by Extension of the Lithosphere[J]. Journal of Petrology, 29(3): 625−679.

Mckenzie D, O'Nions R K. 1991. Partial Melt Distributions from Inversion of Rare Earth Element Concentrations[J]. Journal of petrology, 32(5): 1021−1091.

Meng Y K, Xu Z Q, Santosh M, Ma X X, Chen X J, Guo G L, Liu F. 2016. Late Triassic crustal growth in southern Tibet: Evidence from the Gangdese magmatic belt[J]. Gondwana Research, 37: 449−464.

Meschede M. 1986. A method of discriminating between different types of mid−ocean ridge basalts and continental tholeiites with the Nb−Zr−Y diagram[J]. Chemical Geology, 56(3/4): 207−218.

Middlemost E A K. 1994. Naming materials in the magma/igneous rock system[J]. Earth−Science Reviews, 37(3/4): 215−224.

Miyashiro A. 1974. Volcanic rock series in island arcs and active continental margins[J]. American Journal of Science, 274: 321−355.

Mo X X, Dong G C, Zhao Z D, Guo T Y, Wang L L, Chen T. 2005. Timing of Magma Mixing in the Gangdisê Magmatic Belt during the India− Asia Collision: Zircon SHRIMP U− Pb Dating[J]. Acta Geologica Sinica, 79(1): 66−76.

Mo X X, Hou Z Q, Niu Y L, Dong G C, Qu X M, Zhao Z D, Yang Z M. 2007. Mantle contributions to crustal thickening during continental collision: Evidence from Cenozoic igneous rocks in southern Tibet[J]. Lithos, 96(1): 225−242.

Mo X X, Niu Y L, Dong G C, Zhao Z D, Hou Z Q, Zhou S, Ke S. 2008. Contribution of syncollisional felsic magmatism to continental crust growth: A case study of the paleogene linzizong volcanic succession in southern Tibet[J]. Chemical Geology, 250 (1): 49−67.

Mo Xuanxue, Dong Guochen, Zhao Zhidan, Zhou Su, Wang Liangliang, Qiu Ruizhao, Zhang Fengqin. 2005. Spatial and temporal distribution and characteristics of granitoids in the Gangdese, Tibet and Implication for Crustal Growth and Evolution[J]. Geological Journal of China Universities, 11(3): 281−290 (in Chinese with English abstract).

Mo Xuanxue, Zhao Zhidan, Deng Jinfu, Dong Guochen, Zhou Su, Guo Tieying, Zhang Shuangquan, Wang Liangliang. 2003. Response of volcanism to the India−Asia Collision[J]. Earth Science Frontiers, 10(3): 135−148 (in Chinese with English abstract).

Mo Xuanxue, Zhao Zhidan, Zhou Su, Dong Guochen, Liao Zhongli. 2007. On the timing of India− Asia continental collision[J]. Geological Bulletin of China, 26(10): 10− 14 (in Chinese with English abstract).

Morel M L A, Nebel O, Nebel−Jacobsen Y J, Miller J S, Vroon P Z. 2008. Hafnium isotope characterization of the GJ− 1 zircon reference material by solution and laser−ablation MC−ICPMS[J]. Chemical Geology, 255(1/2): 231−235.

Othman D B, White W M, Patchett J. 1989. The geochemistry of marine sediments, island arc magma genesis, and crust− mantle recycling[J]. Earth & Planetary Science Letters, 94(1/2): 1−21.

Pan Guitang, Mo Xuanxue, Hou Zengqian, Zhu Dicheng, Li Guangming, Zhao Zhidan, Geng Quanru, Liao Zhongli. 2006. Spatial−temporal framework of the Gangdese Orogenic Belt and its evolution[J]. Acta Petrologica Sinica, 22(3): 521− 533 (in Chinese with English abstract).

Pan G T, Wang L Q, Li R S, Yuan S H, Ji W H, Yin F G, Zhang W P, Wang B D. 2012. Tectonic evolution of the Qinghai− Tibet Plateau[J]. Journal of Asian Earth Sciences, 53(2): 3−14.

Pisarevsky S A, Bylund G. 2006. Palaeomagnetism of 935 Ma mafic dykes in southern Sweden and implications for the Sveconorwegian Loop[J]. Geophysical Journal International, 166: 1095−1104.

Pearce J A, Cann J R. 1973. Tectonic Setting of Basic Volcanic Rocks determined using Trace Element Analyses[J]. Earth and Planetary Science Letters, 19(2): 290−300.

Pearce J A, Norry M J. 1979. Petrogenetic implications of Ti, Zr, Y, and Nb variations in volcanic rocks[J]. Contributions to Mineralogy and Petrology, 69(1): 33−47.

Peate D W, Pearce J A. 1998. Causes of spatial compositional variations in Mariana arclavas: Trace element evidence[J]. The Island Arc, 7: 479−495.

Plank T, Langmuir C H. 1998. The chemical composition of subducting sediment and its consequences for the crust and mantle[J]. Chemical Geology, 145(3/4): 325−394.

Robinson J A C, Wood B J. 1998. The depth of the spinel to garnet transition at the peridotite solidus[J]. Earth & Planetary Science Letters, 164(1/2): 277−284.

Sano T, Hasenaka T, Shimaoka A, Yonezawa C, Fukuoka. T. 2001. Boron contents of Japan Trench sediments and Iwate basaltic lavas, Northeast Japan arc: Estimation of sediment− derived fluid contribution in mantle wedge[J]. Earth & Planetary Science Letters, 186(2): 187−198.

Searle M P, Windley B F, Coward M P, Cooper D J W, Rex A J, Rex D, Li T D, Xiao X C, Jan M Q, Thakur V C, Kumar S. 1987. The closing of Tethys and the tectonics of the Himalaya[J]. Geological Society of America Bulletin, 98(6): 678.

Sklyarov E V, Gladkochub D P, Mazukabzov A M, Menshagin Y V, Watanabe T, Pisarevsky S A. 2003. Neoproterozoic mafic dike swarms of the Sharyzhalgai metamorphic massif, southern Siberian craton[J]. Precambrian Research, 122(1/4): 359−376.

Smithies R H, Champion D C, Sun S S. 2004. Evidence for Early LREE− enriched Mantle Source Regions: Diverse Magmas from the c. 3 · 0 Ga Mallina Basin, Pilbara Craton, NW Australia[J]. Journal of Petrology, 45(8): 1515−1537.

Sun S S, Mcdonough W F. 1989. Chemical and isotopic systematics of oceanic basalts: implications for mantle composition and processes[J]. Geological Society London Special Publications, 42 (1): 313−345.

Tang G J, Wang Q, Wyman D A, Sun M, Zhao Z H, Jiang Z Q. 2013. Petrogenesis of gold−mineralized magmatic rocks of the Taerbieke area, northwestern Tianshan (western China): Constraints from geochronology, geochemistry and Sr− Nd− Pb− Hf isotopic compositions[J]. Journal of Asian Earth Sciences, 74(S1): 113−128.

Tang Juxing, Li Zhijun, Dong Shuyi, Lang Xinghai, Wang Zizheng, Zhang Li, Ling Juan, Guo Na. 2005. Geologic Exploration Report of Tangbai Copper Deposit in Xigaze, Tibet[R]. Chengdu: Chengdu University of Technology, 1−40 (in Chinese).

Taylor S R, Mclennan S M. 1995. The geochemical evolution of the continental crust[J]. Reviews of Geophysics, 33(2): 241−265.

Tian S H, Yang Z S, Hou Z Q, Mo X X, Hu W J, Zhao Y, Zhao X Y. 2017. Subduction of the indian lower crust beneath southern tibet revealed by the post−collisional potassic and ultrapotassic rocks in sw Tibet[J]. Gondwana Research, 41(1): 29−50.

Van Hunen J, Allen M B. 2011. Continental collision and slab break−off: A comparison of 3−D numerical models with observations[J]. Earth & Planetary Science Letters, 302(1/2): 27−37.

Wang C, Ding L, Zhang L Y, Kapp P, Pullen A, Yue Y H. 2016. Petrogenesis of Middle− Late Triassic volcanic rocks from the Gangdese belt, southern Lhasa terrane: Implications for early subduction of Neo− Tethyan oceanic lithosphere[J]. Lithos, 262: 320−333.

Wang Xuhui, Lang Xinghai, Deng Yulin, Cui Zhiwei, Lou Yuming, Han Peng. 2018. Zircon U− Pb geochronology, geochemistry and tectonic implications of the Tangbai porphyritic granite pluton in southern margin of Gangdese, Tibet[J]. Geological Journal of China Universities, 24(01): 41− 55 (in Chinese with English abstract).

Wen D R, Chung S L, Song B, Lizuka Y, Yang H J, Ji J Q, Liu D Y, Gallet S. 2008. Late Cretaceous Gangdese intrusions of adakitic geochemical characteristics, SE Tibet: Petrogenesis and tectonic implications[J]. Lithos, 105(1): 1−11.

Wong A, Ton S Y M, Wortel M J R, 1997. Slab detachment in continental collisionzones: An analysis of controlling parameters[J]. Geophysical Research Letters, 24: 2095−2098.

Woodhead J D, Hergt J M, Davidson J P, Eggins S M. 2001. Hafnium isotope evidence for ‘conservative’ element mobility during subduction zone processes[J]. Earth & Planetary Science Letters, 192(3): 331−346.

Wu C Z, Santosh M, Chen Y J, Samson L M, Lei R X, Dong L H, Qu X, Gu L X. 2014. Geochronology and geochemistry of Early Mesoproterozoic meta- diabase sills from Quruqtagh in the northeastern Tarim Craton: Implications for breakup of the Columbia supercontinent[J]. Precambrian Research, 241: 29−43.

Xu R H, Schärer U, Allègre C J. 1985. Magmatism and Metamorphism in the Lhasa Block (Tibet): A Geochronological Study[J]. The Journal of Geology, 93(1): 41−57.

Xu Y G, Lan J B, Yang Q J, Huang X L, Qiu H N. 2008. Eocene break- off of the Neo- Tethyan slab as inferred from intraplate-type mafic dykes in the Gaoligong orogenic belt, eastern Tibet[J]. Chemical Geology, 255(3/4): 439−453.

Xu Y G, Ma J L, Frey F A, Feigenson M D, Liu J F. 2005. Role of lithosphere−asthenosphere interaction in the genesis of Quaternary alkali and tholeiitic basalts from Datong, western North China Craton[J]. Chemical Geology, 224(4): 247−271.

Yin A, Harrison T M. 2000. Geologic Evolution of the Himalayan-Tibetan Orogen[J]. Annual Review of Earth & Planetary Sciences, 28(28): 211−280.

Yin Tao, Li Wei, Yin Xianke, Zhang Wei, Yuan Huayun, Pei Yalun. 2019. The Early Cretaceous granodiorites in the Aweng Co area, Tibet: Evidence for the subduction of the Bangong Co- Nujiang River oceanic crust to the south[J]. Geology in China, 46(5): 1105−1115 (in Chinese with English abstract).

Yuan H L, Gao S, Dai M N, Zong C L, Günther D, Fontaine G H, Liu X M, Diwu C. 2008. Simultaneous determinations of U−Pb age, Hf isotopes and trace element compositions of zircon by excimer laser- ablation quadrupole and multiple- collector ICP- MS[J]. Chemical Geology, 247(1/2): 100−118.

Yuan H L, Gao S, Liu X M, Li H M, Günther D, Wu F Y. 2004. Accurate U−Pb age and trace element determinations of zircon by laser ablation−inductively coupled plasma−mass spectrometry[J]. Geostandards & Geoanalytical Research, 28(3): 353−370.

Yue Yahui, Ding Lin. 2006. ^{40}Ar/^{39}Ar Geochronology, geochemical characteristics and genesis of the Linzhuou basic dikes, Tibet[J]. Acta Petrologica Sinica, 22(4): 855−866 (in Chinese with English abstract).

Zhang Lixue, Wang Qing, Zhu Dicheng, Jia Lili, Wu Xingyuan, Liu Shengao, Hu Zhaochu, Zhao Tianpei. 2013. Mapping the Lhasa Terrane through zircon Hf isotopes: Constraints on the nature of the crust and metallogenic potential[J]. Acta Petrologica Sinica, 29 (11): 3681−3688 (in Chinese with English abstract).

Zhao J H, Zhou M F. 2007. Geochemistry of Neoproterozoic mafic intrusions in the Panzhihua district (Sichuan Province, SW China): Implications for subduction- related metasomatism in the upper mantle[J]. Precambrian Research, 152(1): 27−47.

Zhao Z D, Mo X X, Dilek Y, Niu Y L, DePaolo D J, Robinson P, Zhu D C, Sun C G, Dong G C, Zhou S, Luo Z H, Hou Z Q. 2009. Geochemical and Sr−Nd−Pb−O isotopic compositions of the post-collisional ultrapotassic magmatism in SW Tibet: Petrogenesis and implications for India intra- continental subduction beneath southern Tibet[J]. Lithos, 113(1/2): 190−212

Zhao Zhidan, Zhu Dicheng, Dong Guochen, Mo Xuanxue, DePaolo Don, Jia Lili, Hu Zhaochu, Yuan Honglin. 2011. The ~54Ma gabbro- graniteintrusive in southern Dangxung area, Tibet: Petrogenesis and implications[J]. Acta Petrologica Sinica, 27(12): 3513−3524 (in Chinese with English abstract).

Zheng Y C, Hou Z Q, Li Q Y, Sun Q Z, Liang W, Fu Q, Li W, Huang K X. 2012. Origin of Late Oligocene adakitic intrusives in the southeastern Lhasa terrane: Evidence from in situ, zircon U- Pb dating, Hf- O isotopes, and whole- rock geochemistry[J]. Lithos, 148(3): 296−311.

Zhu D C, Pan G T, Chung S L, Liao Z L, Wang L Q, Li G M. 2008. SHRIMP zircon age and geochemical constraints on the origin of Lower Jurassic volcanic rocks from the Yeba Formation, southern Gangdese, South Tibet[J]. International Geology Review, 50(5): 442−471.

Zhu D C, Wang Q, Zhao Z D, Chung S L, Cawood P A, Niu Y L, Liu S A, Wu F Y, Mo X X. 2015. Magmatic record of India- Asia collision[J]. Scientific Reports, 5: 14289.

Zhu D C, Zhao Z D, Niu Y L, Dilek Y, Hou Z Q, Mo X X. 2013. The origin and pre- Cenozoic evolution of the Tibetan Plateau[J]. Gondwana Research, 23(4): 1429−1454.

Zhu D C, Zhao Z D, Niu Y L, Mo X X, Chung S L, Hou Z Q, Wang L Q, Wu F Y. 2011. The Lhasa Terrane: Record of a microcontinent and its histories of drift and growth[J]. Earth & Planetary Science Letters, 301(1): 241−255.

Zhu D C, Zhao Z D, Pan G T, Lee H Y, Kang Z Q, Liao Z L, Wang L Q, Li G M, Dong G C, Liu B. 2009. Early cretaceous subduction-related adakite- like rocks of the Gangdese Belt, southern Tibet: Products of slab melting and subsequent melt- peridotite interaction?[J]. Journal of Asian Earth Sciences, 34(3): 298−309.

Zhu Dicheng, Zhao Zhidan, Niu Yaoling, Wang Qing, Yildirim DILEK, Dong Guochen, Mo Xuanxue. 2012. Origin and Paleozoic tectonic evolution of the Lhasa Terrane[J]. Geological Journal of China Universities, 18(1): 1−15 (in Chinese with English abstract).

附中文参考文献

安芳, 朱永峰, 魏少妮, 赖绍聪. 2014. 西北天山京希—伊尔曼德金矿区狮子山次火山岩的年代学、地球化学特征及其地质、成矿意义[J]. 岩石学报, 30(6): 1545−1557.

董国臣, 莫宣学, 赵志丹, 朱弟成, 宋云涛, 王磊. 2008. 西藏冈底斯南带辉长岩及其所反映的壳幔作用信息[J]. 岩石学报, 24(2): 203−210.

董铭淳, 赵志丹, 朱弟成, 刘栋, 董国臣, 莫宣学, 胡兆初, 刘勇胜, 邹子昊. 2015. 西藏林周盆地中酸性脉岩的年代学、地球化学和岩石成因[J]. 岩石学报, 31(5): 1268−1284.

高永丰, 侯增谦, 魏瑞华, 孟祥金, 胡华斌. 2006. 冈底斯基性次火山岩地球化学和Sr-Nd-Pb同位素: 碰撞后火山作用亏损地幔源区的约束[J]. 岩石学报, 22(3): 547-557.

耿全如, 潘桂棠, 金振民, 王立全, 朱弟成, 廖忠礼. 2005. 西藏冈底斯带叶巴组火山岩地球化学及成因[J]. 地球科学——中国地质大学学报, 30(6): 747-760.

黄宝春, 陈军山, 易治宇. 2010. 再论印度与亚洲大陆何时何地发生初始碰撞[J]. 地球物理学报, 53(9): 2045-2058.

黄丰, 许继峰, 陈建林, 康志强, 董彦辉. 2015. 早侏罗世叶巴组与桑日群火山岩:特提斯洋俯冲过程中的陆缘弧与洋内弧?[J]. 岩石学报, 31(7): 2089-2100.

侯可军, 李延河, 邹天人, 曲晓明, 石玉若, 谢桂青. 2007. LA-MC-ICP-MS锆石Hf同位素的分析方法及地质应用[J]. 岩石学报, 23(10): 2595-2604.

贾黎黎, 王青, 朱弟成, 陈越, 吴兴源, 刘盛遨, 郑建平, 赵天培. 2013. 重新认识西藏林周盆地基性岩石的地球动力学含义[J]. 岩石学报, 29(11): 3671-3680.

刘彬, 马昌前, 蒋红安, 郭盼, 张金阳, 熊富浩. 2013. 东昆仑早古生代洋壳俯冲与碰撞造山作用的转换:来自胡晓钦镁铁质岩石的证据[J]. 岩石学报, 29(6): 2093-2106.

刘立文, 李建峰, 夏斌, 邱亮斌, 黄强太. 2012. 西藏那木如辉绿岩岩脉的年代学和地球化学特征[J]. 矿物岩石地球化学通报, 31(2): 114-120.

莫宣学, 董国臣, 赵志丹, 周肃, 王亮亮, 邱瑞照, 张风琴. 2005. 西藏冈底斯带花岗岩的时空分布特征及地壳生长演化信息[J]. 高校地质学报, 11(3): 281-290.

莫宣学, 赵志丹, 邓晋福, 董国臣, 周肃, 郭铁鹰, 张双全, 王亮亮. 2003. 印度-亚洲大陆主碰撞过程的火山作用响应[J]. 地学前缘, 10(3): 135-148.

莫宣学, 赵志丹, 周肃, 董国臣, 廖忠礼. 2007. 印度—亚洲大陆碰撞的时限[J]. 地质通报, 26(10): 10-14.

潘桂棠, 莫宣学, 侯增谦, 朱弟成, 王立全, 李光明, 赵志丹, 耿全如, 廖忠礼. 2006. 冈底斯造山带的时空结构及演化[J]. 岩石学报, 22(3): 521-533.

唐菊兴, 李志军, 董树义, 郎兴海, 王子正, 张丽, 凌娟, 郭娜. 2005. 西藏日喀则市汤白铜矿地质勘查报告[R]. 成都: 成都理工大学, 1-40.

王旭辉, 郎兴海, 邓煜霖, 崔志伟, 娄渝明, 韩鹏. 2018. 西藏冈底斯南缘汤白斑状花岗岩锆石U-Pb年代学、地球化学及地质意义[J]. 高校地质学报, 24(1): 41-55.

尹滔, 李威, 尹显科, 张伟, 袁华云, 裴亚伦. 2019. 西藏阿翁错地区早白垩世花岗闪长岩——班公湖—怒江洋壳南向俯冲消减证据[J]. 中国地质, 46(5): 1105-1115.

岳雅慧, 丁林. 2006. 西藏林周基性岩脉的^{40}Ar/^{39}Ar年代学、地球化学及其成因[J]. 岩石学报, 22(4): 855-866.

张立雪, 王青, 朱弟成, 贾黎黎, 吴兴源, 刘盛遨, 胡兆初, 赵天培. 2013. 拉萨地体锆石Hf同位素填图: 对地壳性质和成矿潜力的约束[J]. 岩石学报, 29(11): 3681-3688.

赵志丹, 朱弟成, 董国臣, 莫宣学, DEPAOLO Don, 贾黎黎, 胡兆初, 袁洪林. 2011. 西藏当雄南部约54Ma辉长岩-花岗岩杂岩的岩石成因及意义[J]. 岩石学报, 27(12): 3513-3524.

朱弟成, 赵志丹, 牛耀龄, 王青, Yildirim DILEK, 董国臣, 莫宣学. 2012. 拉萨地体的起源和古生代构造演化[J]. 高校地质学报, 18(1): 1-15.